

**POLITECNICO DI TORINO**

**Master's Degree in Mechatronics**



**Master's Degree Thesis**

# **Recursive Estimation of Wave Spectrum**

**Supervisors**

**Prof. Giuseppe GIORGI**

**Candidate**

**Daniel Andrés MONTOYA ESPINOSA**

**February 13, 2023**



# Summary

This investigation project consist in the emergence of a novel technique for continuous spectrum estimation based on a recursive approach in which the spectrum estimation will be continuously corrected implementing an Extended-Kalman Filter. In order to investigate a bond between the control theory and oceanography, enhancing and modernize the wave spectrum estimation.

It was used the Extended-Kalman Filter (EKF) cyclical procedure, after had have analyzed the results. In this path was considered the stochastic behaviour of the ocean based on JONSWAP spectrum and also implementing a linearization to the model that allowed to obtain a narrow band spectra evaluating each frequency at the time on the basis of the contributing to reduce the complexity of the state-space model at the time, because it was used constant frequencies.

It was opted chose the Least-Squares spectral approximation based on JONSWAP spectrum because it would give a formal solution that helped to model a State-space based of on a cascade of two second order filter and considering the basic principles of a stochastic signal processing in order to implement the robust control technique that allowed to correctly predict the JONSWAP spectrum.

After setting the State-Space model for the EKF (Plan model P-M), another State-space model was prepared (Nominal Model N-M) using the same procedure as for the P-M in order to check the behaviour of the control technique when it was introduced not only similar conditions but also different. The estimation error obtained in each of the performed tests where significantly low, around of 0.094848, when analysing the P-M and N-M in equal conditions, reveling the accurate behaviour that the EKF presented. In the other hand the MSE from the analysis of P-M and N-M in different conditions exhibit a good performance. Also it was deducted that the JONSWAP shape parameter that generated a significant increase in the overall MSE, was the  $H_s$  (significant wave height).

Finally in this investigation was observed that the most remarkable result was the performance of the EKF into the JONSWAP spectrum estimation, revealing that each of the obtained realization was desirable as realistic sea waves under this conditions evaluated.

# Acknowledgements

I am extremely grateful to the IFP - Energies nouvelles, to give this opportunity to be part of such an important research specially with the knowledge and expertise shared with me.

I am also grateful to the Politecnico di Torino - Italy and the Universidad Tecnológica de Bolívar - Colombia to have guided me along my academic path.

Finally, I would like to recognize Patricia Espinosa Lopez, my mother, which have been contributing not only emotional support but also guidance, appreciation, love and discipline for the science and researching.

*“If you’re going to try, go all the way. Otherwise, don’t even start. This could mean losing girlfriends, wives, relatives and maybe even your mind.”*  
*Charles Bukowski,*



# Table of Contents

<b>List of Tables</b>	VIII
<b>List of Figures</b>	IX
<b>Acronyms</b>	XII
<b>1 Introduction</b>	1
1.1 Motivation . . . . .	1
1.2 Previous Work . . . . .	2
1.3 Objectives . . . . .	3
1.4 Work content . . . . .	3
<b>2 Literature review</b>	5
2.1 Introduction . . . . .	5
2.2 Gaussian Description of Ocean Waves . . . . .	5
2.2.1 Gaussian Description Ocean Waves . . . . .	5
2.2.2 Spectral density function . . . . .	5
2.2.3 Wave severity . . . . .	6
2.2.4 Pierson-Moskowitz spectrum . . . . .	6
2.2.5 JONSWAP spectrum . . . . .	6
2.2.6 Wiener-Khintchine theorem . . . . .	7
2.3 Statistical Fundamentals . . . . .	7
2.3.1 Stochastic Process . . . . .	7
2.3.2 Markov Process . . . . .	8
2.3.3 Least Squares . . . . .	8
2.3.4 Steady-state ergodic random process . . . . .	8
2.3.5 Correlation . . . . .	8
2.3.6 Auto-Correlation . . . . .	8
2.3.7 White noise signal . . . . .	9
2.3.8 Covariance Function . . . . .	10
2.3.9 Confidence Interval . . . . .	10

2.4	Control Analysis Fundamentals . . . . .	11
2.4.1	State space model . . . . .	11
2.4.2	Controllability . . . . .	11
2.4.3	Observability . . . . .	11
2.4.4	Sample time . . . . .	11
2.4.5	Aliasing . . . . .	11
2.4.6	Shannon's theorem . . . . .	12
2.4.7	Spectrogram . . . . .	12
2.4.8	Kalman filter . . . . .	12
2.4.9	Extended Kalman Filter EKF . . . . .	15
<b>3</b>	<b>Methods</b>	<b>16</b>
3.1	Introduction . . . . .	16
3.2	Least-Squares Spectral Approximation - LS . . . . .	16
3.2.1	Initial Conditions . . . . .	18
3.3	Response of the System to Random Inputs . . . . .	19
3.3.1	State- Space Modelling . . . . .	19
3.3.2	Stochastic signal processing . . . . .	24
3.3.3	Bandwidth selection . . . . .	25
3.3.4	Low Pass Filter (LPF) Design . . . . .	25
3.3.5	Stability and Steady state analysis . . . . .	27
3.4	Kalman Filter Design . . . . .	27
3.4.1	Prediction step . . . . .	28
3.4.2	Correction Step . . . . .	29
3.4.3	Block diagram scheme . . . . .	29
<b>4</b>	<b>Results and Discussion</b>	<b>31</b>
4.1	Calculation Procedure Setup . . . . .	31
4.1.1	Equivalent conditions . . . . .	31
4.1.2	Different conditions . . . . .	33
4.1.3	MSE analysis - Varying JONSWAP shape parameters in plant model (P-M) . . . . .	43
4.2	Results Comparison . . . . .	44
4.2.1	Analysis at different conditions . . . . .	44
4.2.2	MSE - Analysis . . . . .	46
<b>5</b>	<b>Conclusion and Potentially Future Work</b>	<b>48</b>
5.1	Future Work . . . . .	48
<b>A</b>	<b>Attestation de Stage</b>	<b>50</b>
<b>B</b>	<b>Extended - Kalman Filter MATLAB code implementation</b>	<b>51</b>

<b>C Least-Squares MATLAB code implementation</b>	<b>59</b>
<b>Bibliography</b>	<b>62</b>

# List of Tables

3.1	Initial conditions - Fitted Parameters . . . . .	18
4.1	Assumed spectrum parameters - Nominal model . . . . .	31
4.2	Different test varying the JONSWAP spectrum shape parameters with respect the N-M . . . . .	45

# List of Figures

2.1	White noise representation - A) time domain B) frequency domain . . . . .	9
2.2	Critical values of the standard normal distribution . . . . .	10
3.1	Gain and Critical Damping Ratio vs Peak Enhancement factor ( $\gamma$ ) . . . . .	18
3.2	Fitting parameter vs Peak Enhancement factor ( $\gamma$ ) . . . . .	19
3.3	Fitting parameter vs Peak Enhancement factor ( $\gamma$ ) - Initial conditions . . . . .	20
3.4	Spectral density function - Target spectrum and Approximate spectrum $H_s = 1, \gamma = 2$ and $T_p = 10$ . . . . .	21
3.5	Spectral density function - Approximate spectrum and Target Spectrum . . . . .	24
3.6	Spectrogram - $\gamma = 5$ $H_s = 5$ $T_p = 10$ . . . . .	25
3.7	SDF comparison . . . . .	26
3.8	Zero and Poles locations . . . . .	27
3.9	Step response . . . . .	28
3.10	Block diagram Scheme . . . . .	29
4.1	Target and Estimated realizations - Equivalent conditions . . . . .	32
4.2	P-M Target Spectrum, Kalman filter - Estimated Spectrum - Equivalent conditions . . . . .	32
4.3	State Variable $\dot{x}_2$ - Equivalent conditions . . . . .	33
4.4	a)Target and Estimated realizations b)Spectrum c)State Variable $\dot{x}_2$ - P-M conditions $H_s = 1.1, \gamma=2, T_p=10$ . . . . .	34
4.5	a)Target and Estimated realizations b)Spectrum c)State Variable $\dot{x}_2$ - P-M conditions $H_s = 1, \gamma=2,5 T_p=11$ . . . . .	35
4.6	a)Target and Estimated realizations b)Spectrum c)State Variable $\dot{x}_2$ - P-M conditions $H_s = 1.1, \gamma=2,5 T_p=11$ . . . . .	36
4.7	a)Target and Estimated realizations b)Spectrum c)State Variable $\dot{x}_2$ - P-M conditions $H_s = 1, \gamma=2,5 T_p=10$ . . . . .	37
4.8	a)Target and Estimated realizations b)Spectrum c)State Variable $\dot{x}_2$ - P-M conditions $H_s = 1, \gamma=2 T_p=11$ . . . . .	38
4.9	a)Target and Estimated realizations b)Spectrum c)State Variable $\dot{x}_2$ - P-M conditions $H_s = 2, \gamma=3 T_p=11$ . . . . .	39

4.10	a)Target and Estimated realizations b)Spectrum c)State Variable $\dot{x}_2$ - P-M conditions Hs = 3 $\gamma=3.3$ Tp=12 . . . . .	40
4.11	a)Target and Estimated realizations b)Spectrum c)State Variable $\dot{x}_2$ - P-M conditions Hs = 1 $\gamma=3$ Tp=10 . . . . .	41
4.12	a)Target and Estimated realizations b)Spectrum c)State Variable $\dot{x}_2$ - P-M conditions Hs = 3 $\gamma=2$ Tp=10 . . . . .	42
4.13	a)Target and Estimated realizations b)Spectrum c)State Variable $\dot{x}_2$ - P-M conditions Hs = 1 $\gamma=2$ Tp=12 . . . . .	43
4.14	MSE - Varying Hs . . . . .	44
4.15	MSE - Varying Tp . . . . .	45
4.16	MSE - Varying $\gamma$ . . . . .	46
A.1	Attestation de Stage . . . . .	50



# Acronyms

**JONSWAP spectrum**

Joint North Sea Wave Observation Project Spectrum

**ACF**

Auto-correlation Function

**SDF**

Spectral density function

**N-M**

Nominal Model

**P-M**

Plant Model

**LPF**

Low-Pass-Filter

# Chapter 1

## Introduction

### 1.1 Motivation

Over the years the interest of finding more sustainable ways of buying energy has a concern, specially in the need to lessen reliance on fossil fuels and the resources of other entities.

Oceans offer significant potential for renewable energy production on the route to de-carbonizing of the energy mix, including offshore wind, tides, waves, temperature and salinity gradients. However, the water is a demanding environment that poses a serious challenge to both equipment and structures. In particular, waves play a crucial role in determining whether or not many maritime operations are feasible since they pose both a significant threat and a potential source of energy. Ocean waves take on a wide variety of shapes, making them a rich scientific subject for research in disciplines like hydrodynamics, applied mathematics, statistical physics, or oceanography.

In the path of understanding the different phenomena of the ocean is crucial to investigate a novel technique for continuous spectrum estimation based on a recursive method in which the spectrum estimation will be continuously corrected in the manner of an adaptive Kalman filter using the differences observed in real time between, on the one hand, the sensor measurements, and, on the other hand, those expected given the current spectrum estimation. By establishing a fresh link between control theory and oceanography, this method seeks to modernize and strengthen spectrum estimation.

## 1.2 Previous Work

The majority of the previous wave spectrum estimation research has been done on prediction the surface elevation. One method based on spatial prediction of wave elevation through physical or stochastic propagation models at a given point can then be seen as the sum of cosines with various frequencies and phases, using one or more observations in the area of the point of interest. As a result, recursive models for representing waves were developed.

Additionally, there is another method in which the sea elevation is then divided into a number of components with various selected frequencies. Only considering previous measurements made at the point of interest; these techniques treat the wave elevation as a time series, with each frequency component's phase and amplitudes being determined by resolving a least squares problem using the initial data and a Kalman filter is latter applied to the model as developed in the article "Filter Approaches to wave kinematics approximations" of P-T. D. Spanos and "Constrained Optimal Control of a Heaving Buoy Wave-Energy Converter" Hels et al.

The selection of the harmonic component frequencies and their distribution within the range is crucial in those recursive approaches. A uniform distribution over the range is the most reliable option because it won't be significantly impacted by a change in the wave spectrum. The frequencies are constant in time and are not easily determinable. These two issues are addressed by Kalman filter and auto-regressive models.

Also, P-T. D. Spanos Implements the auto-regressive models [1], in which is presented three different algorithms for simulating a time series that is appropriate for a specific power spectrum of ocean waves but only focusing in a sum of a linear combination of previous values and a linear combination of white noise deviates.

In the other hand Budal and Falnes [2] have implemented the Kalman Filter to adaptively calculate, based on remote pressure data, the frequency, phase and amplitude of the wave excitation force acting on a heaving body. The validity of these very rigorous simplifying hypothesis, which call for simple sinusoidal behavior of the excitation force and mono-directional wave propagation, is not evaluated in actual sea conditions.

A wave prediction using linear digital filters and inputs of either distant pressure measurements or distant wave height was proposed in more recent solutions. However, the intrinsically behaviour of the waves, is crucial treating it as a non linear problem.

## 1.3 Objectives

- The main research direction for this thesis is to contribute with the recursive estimation implementing a Extended-Kalman Filter clearly formulated. Analyzing numerically the obtained results in order to implement estimators and variations in the co-variances matrices in order to generate an extended Kalman Filter and adapted.
- The analysis is fitted by applying the stochastic behaviour of the ocean. While estimating the ocean spectrum in real conditions and for sake of simplicity implement a linearization to the model that allows to obtain a narrow band spectra by means of the recursive analysis of the evaluated frequencies.
- The response of the Kalman Filter incorporates an optimization in diverse conditions taking into consideration the confident intervals for a normal and gaussian likelihood.

## 1.4 Work content

The following investigation is divided in five chapters, in which the introduction is the first.

**Chapter 2: Literature Review.** In the following chapter is introduced the basic and implemented literature about Gaussian description of ocean waves, statistical fundamentals and control analysis fundamentals.

**Chapter 3: Methods** In this chapter is presented the methodology followed, Starting from the Least-Squares spectral approximation, subsequently the state space model is defined. Then, the previously state-space is excited with a unit intensity white-noise signal input to extract the JONSWAP spectrum and before introducing it into the extended-kalman filter (EKF) it necessary to pre process the signal by selecting its frequency bandwidth and applying a Low pass filter in order to create a discrete signal ready to be used in the EKF. Finally the EKF is designed taking into account some considerations.

**Chapter 4: Results and Discussion** The main quality criterion used to state if the EKF is performing quiet approximated narrow estimations is the confidence interval. Also it is used the MSE calculation along variation of the plan model

(P-M), meaning that the approximation done by the filter kalman can be considered as well performed.

**Chapter 5: Conclusion and Potentially future work** In this last chapter is summarized all the obtained results. And it is given some considerations in order to continue improving not only the estimation of the JONSWAP spectrum but also the different other types existing.

**Appendix A: Attestation de Stage** Here is presented the company in where I performed and acquire a wide view of this field and all the required tools to develop my investigation.

**Appendix B: Extended - Kalman Filter MATLAB code implementation** The equations, algorithms and calculations used along the developing of the Extended-Kalman filter are gathered in this appendix.

**Appendix C: Least-Squares MATLAB code implementation** The Least-Square spectral approximation equation, algorithms and calculation are used in the following appendix.

# Chapter 2

## Literature review

### 2.1 Introduction

In this chapter is for introduce to the reader the concepts needed to understand the wave prediction. First, it outlines the basics of ocean wave descriptions.

### 2.2 Gaussian Description of Ocean Waves

#### 2.2.1 Gaussian Description Ocean Waves

Ocean waves can be observed as Gaussian random process, waves are steady-state, ergodic random process for which the probability distribution of displacement from the mean value (namely wave profile), follows the normal probability law with zero mean and a variance representing the sea severity [3].

#### 2.2.2 Spectral density function

Representation of potential and kinematic energies of random waves, also known as the wave spectrum. Often significant role in evaluating the statistical properties of stochastic waves.

The magnitude of the auto-correlation function for any time  $t$  represents the time average of the wave energy [3].

It is also possible to express the average energy of a wave in frequency domain applying the Fourier transform for  $x(t)$  obtaining  $X(w) = \int_{-\infty}^{\infty} |x(t)e^{-iwt} dt$  by the Parseval theorem (Eq.2.1).

$$\int_{-\infty}^{\infty} x(t)^2 dt = \frac{1}{2\pi} \int_{-\infty}^{\infty} \int_{-\infty}^{\infty} |x(t)e^{-iwt} dt|^2 dw \quad (2.1)$$

Moreover, is possible to interpret according to the properties of the auto-correlation function that, the area under the curve from spectrum is also equal to the variance of waves. By this, in order to have a proper representation of the spectral density distribution for ocean waves, it is defined as follows:

$$S_{xx} = \lim_{T \rightarrow \infty} \frac{1}{2T} |X(w)|^2 \quad (2.2)$$

### 2.2.3 Wave severity ( $H_s$ )

Expressed as the wave height of the spectrum, is equal to four times the square-root of the area under the curve of the spectral density function.

### 2.2.4 Pierson-Moskowitz spectrum

This formulation was obtained from the analysis of measured data obtained in the North Atlantic in 1964. Proposing that if the wind blew steadily for a long time over a large are, the waves would come into equilibrium with the wind. Which is a concept of fully developed sea, e.g under a given constant wind speed a state of energy saturation in which a balance is set up from a rate at which the energy is increase from the wind and the rate at energy lost[4].

$$S(w) = \frac{\alpha g^2}{w^5} \exp \left[ -\beta \left( \frac{w_o}{w} \right)^4 \right] \quad (2.3)$$

In order to obtain a better approximation the following constant from the Eq.2.3 must be follow as,  $\alpha = 8.1 \times 10^{-3}$ ,  $\beta = 0.74$ ,  $w_o = g/U$  and  $U$  is the wind speed at a height of 19.5 m above the sea surface [5].

### 2.2.5 JONSWAP spectrum

Wave measurement program known as the Joint North Sea Wave Project carried out in 1968 and 1969 along a line extending over 160 km into the North Sea from Sylt Island. The spectrum represents the wind-generated seas which fetch limitation, and wind speed and fetch length are inputs to this formulation.[3]

$$S_{(f)} = \alpha \frac{g^2}{(2\pi)^4} \frac{1}{f^5} - 1.25 \left( \frac{f_m}{f} \right)^4 \gamma^{\exp[-(f-f_m)^2/2(\sigma f_m)^2]} \quad (2.4)$$

Be  $f$  the wave frequency,  $g$  the constant of gravity,  $f_m = 3.5(g/\tilde{U})$  modal frequency,  $\tilde{U}$  wind speed,  $\alpha = 0.076x^{(-0.22)}$  dimensionless fetch length,  $x$  fetch

length and  $\sigma = 0.07$  for  $f \leq f_m$  and  $0.09$  for  $f > f_m$ .

This theoretical model is obtained by the measuring of the rough North sea but not only is implemented in this regions but also in geographically specific locations where it is important to obtain the characteristic wave frequency.

## 2.2.6 Wiener-Khintchine theorem

Wiener theorem is used in the analysis of stochastic analysis of random waves mainly on the relation that exist between between the auto-correlation function (Eq.2.5) defined in time domain and the Spectral Density Function (SDF) (Eq.2.6) defined in the frequency domain. Both are the Fourier transform of each other[6].

$$R_{xx}(\tau) = \frac{1}{\pi} \int_{-\infty}^{\infty} S_{xx}(w) e^{-i\omega\tau} d\omega \quad (2.5)$$

$$S_{xx}(w) = \frac{1}{\pi} \int_{-\infty}^{\infty} R_{xx}(\tau) e^{-i\omega\tau} d\tau \quad (2.6)$$

Thus, having the spectral density function such the area under  $S_{xx}(w)$  is equal to the variance of  $x(t)$ .

$$\int_0^{\infty} S_{xx}(w) dw = R_{xx}(0) = Var[x(t)] \quad (2.7)$$

## 2.3 Statistical Fundamentals

### 2.3.1 Stochastic Process

Also known as random process, can be defined as a group of variables  $x(t, w)$ ,  $t \in T \wedge w \in W$ . Considering variable  $t$  as time and  $w$  as sampled space. This random function can be seen either as discrete time process or a continuous time process. And  $x(t, \cdot)$  are random values obtained in space (state space), while fixing  $x(\cdot, w)$  obtaining the sample function trajectory which is the single outcome of a stochastic process [7].

This is associated to the impossibility to find the probability measure to all subsets of  $W$ . By this each probability and stochastic process are associated only with the value in each set.

### 2.3.2 Markov Process

Is considered as a stochastic model in which are described a sequence of events in which the probability of an event, depend only on the state of the last event and not in any other state in the past (memory-less property) [8].

### 2.3.3 Least Squares

The least-square method finds the optimal parameter values by minimizing the sum of squared residuals [9].The residuals considered as the observed value of the dependent function  $S(f)$  and the value predicted by the model  $\hat{S}(f)$ .

$$F = \min \Sigma [S(f) - \hat{S}(f)]^2 \quad (2.8)$$

The objective is principally to adjust the parameters from an estimated function model from a initial function model in order to fit in the best way a estimated model.

### 2.3.4 Steady-state ergodic random process

An aleatory signal that does not change its statistical behaviour during the time is considered as steady-state random process. And the ergodicity of an aleatory signal is present only if one realization represents all the rest, also the ergodicity only will be present in stationary processes[10].

As a result a random process is said to be ergodic in auto-correlation , if time averaged auto-correlation if time averaged in ACF is equal to ensemble averaged ACF.

### 2.3.5 Correlation

The correlation helps to obtain the information of how different set of variables are associated being possible to obtain information from a variables just knowing the previous one.

$$r = \frac{Cov(Z(x), Z(y))}{\sigma_{Zx}\sigma_{Zy}} \quad (2.9)$$

### 2.3.6 Auto-Correlation

As state previously the variance can give the information of how much noise is presented in a signal. To analyse this behaviour not only over the time but also on the frequency domain is used the ACF.

The auto-correlation function (Eq. 2.10) is essentially a covariance function, on account of the weakly steady-state condition, the covariance function for any given time  $t$  and  $t + \tau$  will only depend on the time difference  $\tau$ . The ACF is defined to produce the variance of the stochastic waves in the time domain, also it is usefully for transferring from the time domain to the frequency domain[11].

$$R_{xx}(\tau) = \lim_{T \rightarrow \infty} \frac{1}{2T} \int_{-T}^T x(t)x(t + \tau) dt \quad (2.10)$$

Also, Eq.2.10 expressed in the time domain, can be used in the frequency domain applying a temporal-spectral relationship known as the Wiener-Khintchine theorem Eq. 2.5 and Eq. 2.6

### 2.3.7 White noise signal

For a given random signal in which its ACF is  $\delta(\tau)$  (dirac delta function) having  $R_{xx} = 0$  every where except on  $\tau = 0$ . Taking into account that the ACF will be represented as "dirac" pulse, its Fourier transform is equivalent to a constant frequency spectrum (Fig 2.1).

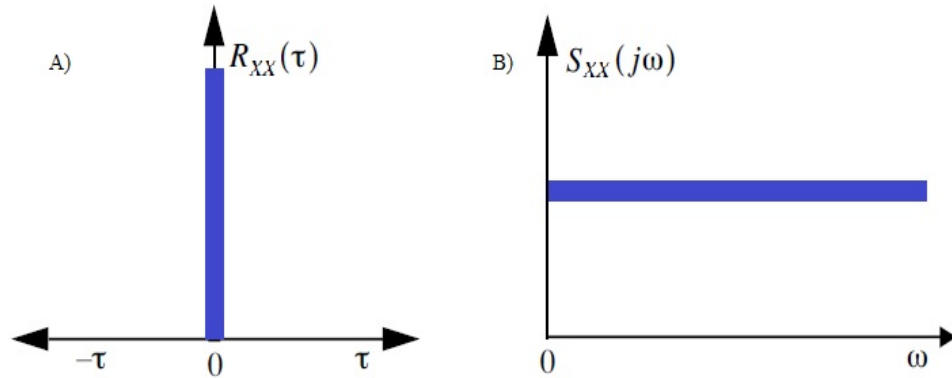


**Figure 2.1:** White noise representation - A) time domain B) frequency domain

Also, a white noise signal is independent, because at any sample time signal it is completely uncorrelated from any other sample time signal.

Often signal can be filter out the white noise source to achieve a non-white noise or colored noise source limited in a specific frequency bandwidth and correlated domain.

### 2.3.8 Covariance Function

Having two stochastic processes  $Z(x), t \in T \wedge Z(y), t \in Y$  the covariance function will express how much these two stochastic variables will change [12]. The covariance function will be express as:

$$Cov[Z(x), Z(y)] = E[Z(x) - E(Z(x))][Z(y) - E(Z(y))]^T \quad (2.11)$$

Consequently shows a dependency measure between values from the stochastic process in different  $T$  instant, providing information of its variations. In the case it is obtained that  $Z(x), t \in T \wedge Z(y), t \in Y$  are the same, this situation must be considered as auto-covariance function, where  $\mu$  corresponds to the mean of each random process.

$$Cov[Z(x), Z(y)] = E[(Z(x) - \mu_x)(Z(y) - \mu_y)] \quad (2.12)$$

### 2.3.9 Confidence Interval

In a range of possible values of estimates, it is important to create confidence intervals in order to define how confident the measurement is with respect to the true parameter value is likely to be in this interval [9].

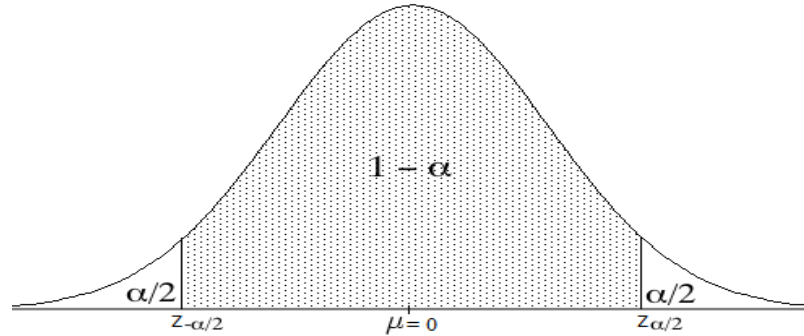


**Figure 2.2:** Critical values of the standard normal distribution

In Figure 2.2, the two symmetric values ( $Z_{\pm\alpha/2}$ ) with respect to the mean of a normal distribution  $Z \sim N(0,1)$ . The area under the curve  $1 - \alpha$  represents the probability to fall in this interval. The remaining sections of the curve  $\alpha/2$  corresponds to the probability to be outside the confidence level.

$$Z = \frac{X - \mu}{\sigma} \quad (2.13)$$

The standard score (Eq.2.13), allow to normalize a given a random process  $X \sim N(\mu, \sigma^2)$  at designated confidence level.

## 2.4 Control Analysis Fundamentals

### 2.4.1 State space model

A set of mathematical dynamic equations with multiple input/output which represents a physical dynamic system, utilizing first-order differential equations. The representation in continuous-time (2.14) and discrete-time are (2.15) [13]:

$$\begin{aligned} \dot{x} &= Ax + Bu \\ y &= Cx + Du \end{aligned} \tag{2.14}$$

$$\begin{aligned} \dot{z}_t &= Az_t + Bu_t \\ y_t &= Cz_t + Du_t \end{aligned} \tag{2.15}$$

### 2.4.2 Controllability

Refers to a system by means of an unconstrained control vector that is possible to be transferred from any initial state  $x(t_0)$  to any other state in a finite interval of time.[14]

### 2.4.3 Observability

Refers to a system in any time  $t_0$  in which is possible to determine this state from the observation of the output over a finite time interval [14]. Indeed, measures how properly the intrinsic states of a dynamic system perturb the acquisition of the outputs.

### 2.4.4 Sample time

Refers to the rate rate at which a discrete systems samples its inputs.

The effect of ideal sampling time is to replicate the

### 2.4.5 Aliasing

The aliasing is phenomenon generated from the conversion from analog to discrete domain (i.e. an alias of the sampled signal is reconstructed) and may occur for any type of signal if the sampling rate is not properly chosen.

### 2.4.6 Shannon's theorem

In order to avoid aliasing effect, is need to understand the aliasing effect. For this when a spectrum  $S_{(w)}$  is needed to be sampled, its signal bandwidth must be defined as:

$$w_- = \min w : |S_w| \neq 0 \wedge w_0 = \max w : |S_w| \neq 0 \wedge w_b = w_0 - w_- \rightarrow w_0 < \infty \quad (2.16)$$

A signal is said to be band-limited if its amplitude spectrum goes to zero for all frequencies beyond some threshold called the cutoff frequency  $w_0$ . The ideal sampling frequency  $w_s$  is to replicate the original spectrum as:

$$w_s > 2w_0 \rightarrow w_0 < \frac{w_s}{2} = w_n \rightarrow \text{NyquistFrequency} \quad (2.17)$$

### 2.4.7 Spectrogram

The spectrogram based on the short-time Fourier transform was proposed a tool to study the time frequency evolution of the properties of ocean wind waves [15].

This mathematical tool provides a proper representation of the averaged frequencies, evaluating in frames (signal chunks) across the whole duration of the random realization. This will contribute to obtain the amount of power spectral density and also determine from which point the the signal has low amplitudes.

### 2.4.8 Kalman filter

The Kalman filter algorithm is a mathematical tool that contributes to the estimation of unknown variables, taking into account observed data during certain period of time. Also can be used for stochastic estimation from noisy sensor measurements.

The Kalman filter is essentially a set of mathematical equations that implement a predictor-corrector type estimator that is optimal in the sense that it minimizes the estimated error covariance [16].

This algorithm has to steps, one is related to the time update and the second is measurement which is sub-divided in two other steps called prediction and correction.

The the state-space model is developed the estimation of the state  $x \in R^n$  of a discrete-time controlled process that is obtained by the linear stochastic equation.

$$x_t = Ax_{t-1} + Bu_{t-1} + w_{t-1} \quad (2.18)$$

$$z_t = Hx_t + v_t \quad (2.19)$$

Knowing that  $n$  are the number of states in the system,  $r$  is the dimensionality of the control commands (inputs) and  $m$  are the number of observations in the system (outputs)

- $A$  -  $n \times n$  matrix that describes how the state evolves from  $t - 1$  to  $t$  without controls or noise.
- $B$  -  $n \times r$  matrix that describes how the control  $u_t$  changes the state from  $t_1$  to  $t$ .
- $H$  -  $m \times n$  matrix that describes how the state variables  $x_t$  are mapped into a response of the system  $z_t$ .
- $w_{t-1}$ ,  $v_t$  - Random variables that represent the process and measurement noise which are assumed as independent and normally distributed (white noise) with covariance  $R$  and  $Q$  respectively.

### Prediction Step

This step is also known as the *time update* step. In which Eq. 2.20 project forward in time the current state an error variance, in order to obtain estimates from the next time step.

$$\hat{x}_t^- = A\hat{x}_{t-1} + Bu_{t-1} \quad (2.20)$$

$$P_t^- = AP_{t-1}A^T + Q \quad (2.21)$$

- $\hat{x}_t^-$  - Represents the prior estimate, that an approximated calculation before the measurement update correction.
- $\hat{x}_t$  - Represents the precedent estimate, that an approximated calculation before the measurement update correction.
- $e_t^- = x_t - \hat{x}_t^-$  - *A priori* estimate error.
- $e_t = x_t - \hat{x}_t$  - *A posteriori* estimate error.
- $P_t^- = E[e_t^- e_t^{-T}]$  - *A priori* error covariance.
- $P_t = E[e_t e_t^T]$  - *A posteriori* error covariance.
- $Q = E[ww^T]$  - Represents the covariance matrix of the Gaussian noise  $w_k$ .

### Correction Step

This step is also known as the *measurement update* step. These equations also contribute to feedback and upgrade and estimate from *a priori* estimate [17].

$$K_t = P_t^- H^T (H P_t^- H^T + R)^{-1} \quad (2.22)$$

$$\hat{x}_t = \hat{x}_t^- + K_t (z_t - H \hat{x}_t^-) \quad (2.23)$$

$$P_t = (I - K_t H) P_t^- \quad (2.24)$$

- $K_t$  - Kalman gain is a  $n \times m$  matrix, is called the gain or blending factor, that minimizes the precedent error covariance equation  $P_k$ .
- $R = E[vv^T]$  - Represents the covariance matrix of the Gaussian noise  $v_k$ .
- $z_t - H \hat{x}_t^-$  - The residual and represents the difference between the predicted measurement  $H \hat{x}_t^-$  and the actual measurement  $z_k$ .

### Calculation Procedure

Starting from the *measurement update*.

- 1- Set initial estimates for  $\hat{x}_{t-1}$  and  $P_{t-1}$ .
- 2- Compute first the Kalman gain  $K_t$  from Eq. 2.22.
- 3- Compute the measurement  $z_k$  from Eq. 2.26.
- 4- Compute the precedent estimate  $\hat{x}_t$  from Eq. 2.23.
- 5- Compute *a posteriori* error covariance  $P_t$  from Eq. 2.24.

Then proceed with *Time update*.

6- Compute next time instant  $t$ , *a priori* error covariance  $P_t^-$  from Eq. 2.21 with obtained  $P_{t-1}$  at previous time instant (starting from initial conditions).

7- Compute the prior estimate  $\hat{x}_t^-$  with the previous precedent estimate  $\hat{x}_t$  based on Eq. 2.20.

- 8- Restart again the calculation procedure.

### 2.4.9 Extended Kalman Filter EKF

Most realistic problems involve nonlinear functions. For this the following linear model (Eq. 2.25 and Eq. 2.26) must be change into a nonlinear model.

$$x_t = Ax_{t-1} + Bu_{t-1} + w_{t-1} \quad (2.25)$$

$$z_t = Hx_t + v_t \quad (2.26)$$

The main problem of using the nonlinear function is that will lead to non-gaussian distributions and the normal kalman filter is not applicable anymore. Thus, the following nonlinear model is considered (Eq. 2.27 and Eq. 2.28) .

$$x_t = g(u_t, x_{t-1}) + w_{t-1} \quad (2.27)$$

$$z_t = h(x_t) + v_t \quad (2.28)$$

To implement EKF is need to apply local linearization based on Taylor which is basically taking a point and computing its partial derivative around this linearization point.

Looking around the prediction step is analysed how far is the actual measurement.

$$g(u_t, x_{t-1}) \approx g(u_t, \nu_{t-1}) + \frac{\partial g(u_t, \nu_{t-1})}{\partial x_{t-1}}(x_{t-1} - \nu_{t-1}) \quad (2.29)$$

Also the correction step is linearized.

$$h(x_t) \approx h(\hat{u}_t) + \frac{\partial h(\hat{u}_t)}{\partial x_t}(x_t - \hat{u}_t) \quad (2.30)$$

Also, is important to remark that the differential term corresponds to the Jacobian, which is the orientation of the tangent plane to the vector-valued function at a given point.

In general aspects the Eq. 2.20 will be follow as:

$$\hat{\nu}_t^- = g(u_t, \nu_{t-1}) \quad (2.31)$$

And Eq.2.23 leads to:

$$\hat{x}_t = \hat{x}_t^- + K_t(z_t - h(\hat{\nu}_t^-)) \quad (2.32)$$

The calculation procedure explained in the above section 2.4.8 Kalman filter, is performed in the same manner but applying the previously changes.

# Chapter 3

## Methods

### 3.1 Introduction

In this chapter will be presented the different methods considered in order to calculate a estimation of the wave spectrum. In first instance, is introduced the different sources of prediction numerical tools. The Least-squares Spectral approximation based on JONSWAP spectrum. Which would give a formal solution in order to implement the robust control technique that will allow to correctly predict the JONSWAP spectrum.

### 3.2 Least-Squares Spectral Approximation - LS

The JONSWAP spectrum is a modification of the Pierson-Moskowitz spectrum as a consequence of fetch limitations and makes it possible to modulate a spectral sharpness (Eq. 3.1).

$$S_{(w)} = \frac{5}{16} \frac{H_s^2 w_m^4}{w^5} \exp \left[ -\frac{5}{4} \left( \frac{w_m}{w} \right)^4 \right] \gamma^{\exp[-(w-w_m)^2/2(\sigma w_m)^2]} \quad (3.1)$$

An approximation obtained for the Pierson-Moskowitz spectrum which was modeled by employing a cascade of two linear second filter by Spanos T-P (Eq. 3.3), which in technical aspects is considered a fourth order filter.

$$H_{j(w)} = \frac{g_1 w^2}{(w^2 - k_1)^2 + (c_1 w)^2} \frac{g_2 w^2}{(w^2 - k_2)^2 + (c_2 w)^2} \quad (3.2)$$

Above expression will be used for JONSWAP spectrum calculation due to the adequacy of the spectral matching for several wind velocities. Eq.3.2 has five fitting

parameters which develop a crucial role at the moment of calculating a specific spectrum.

To have a narrow representation of the JONSWAP the following constraints must be set:

- $g_1, g_2, k_1, k_2, c_1, c_2 \geq 0$  These constraints must be greater than zero in order to guaranty the controllability in the state space system modelling and the stability as well. This procedure was done by mean of control analysis theory in Section 3.3.5.

$$H_j(w) = \frac{Gw^4}{[(w^2 - k_1)^2 + (c_1w)^2][(w^2 - k_2) + (c_2w)^2]} \quad (3.3)$$

- $G$  – Will behave as a gain while the energy spectrum increase. Also it is the product of  $g_1g_2$ .
- $c_1/\sqrt{k_1}, c_2/\sqrt{k_2}$  – Assuming their behaviour as the critical damping ratios [18]. The enhancing of the spectral sharpness  $\gamma$  will be due to the decreasing of the  $c_1/\sqrt{k_1}$  and the increasing of the  $c_2/\sqrt{k_2}$  damping ratios.

The main objective is to obtain a model that allows to predict a JONSWAP spectrum from a data set. By having this model, it is able to adjust the data sets from any others if needed.

Studies for the implementation of ARMA algorithms for ocean wave modelling has been integrated in the sake of simplicity of existence of approximations simpler and logically accurate. Although, the Least-Square method for approximation of the JONSWAP spectrum has been chosen because it is one of the most practical ways for providing a clearly formulated solution ([19]).

$$F = \min \Sigma [S_{(f)} - \hat{S}_j(w)]^2 \quad (3.4)$$

JONSWAP spectrum contributes in certain manner to modify the Pierson-Moskowitz spectrum as a consequence of fetch limitations and it is possible to realize a spectral sharpness, allowing to determine the predominance of certain frequencies. Also it was decided that the approach done for the Pierson-Moskowitz spectrum, employing a cascade of two linear second filter done by Spanos T-P obtaining an spectral coincidence [18].

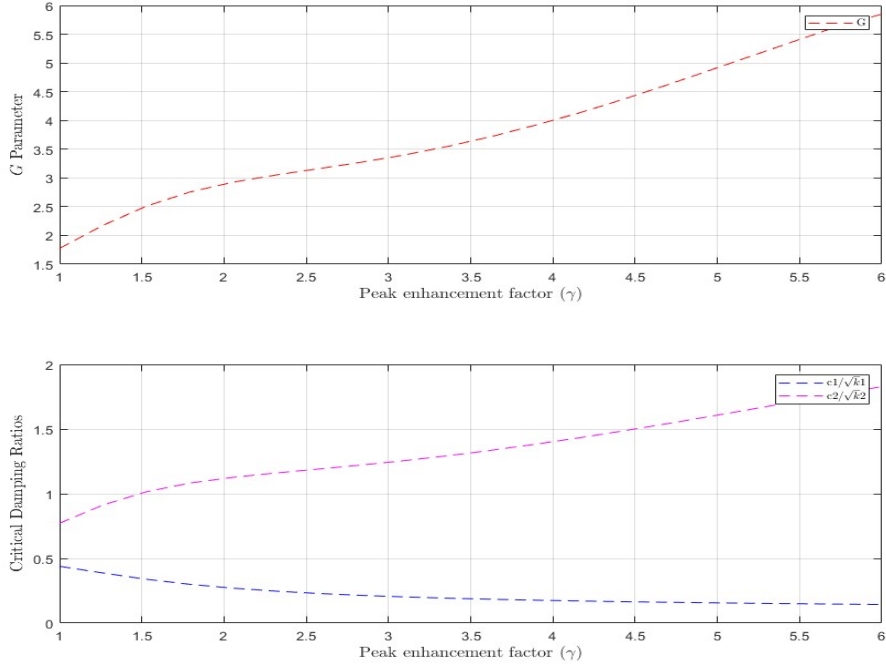


**Figure 3.1:** Gain and Critical Damping Ratio vs Peak Enhancement factor ( $\gamma$ )

### 3.2.1 Initial Conditions

Due to the practical usefulness, the parameters were calculated for values of  $\gamma$  from 1-10. After several iterations and observing the variation of the fitted parameters with respect to the Peak enhancement  $\gamma$  by looking to the different solution from the LS approximation method.

The initial values for the fitted parameters assumed for this model representation are the selected by having a minimum variation with respect of the peak enhancement increase corresponding to  $\gamma = 7$ , the pertinent numerical data are shown:

G	$k_1$	$k_2$	$c_1$	$c_2$
6.183	0.398	1.794	0.085	2.709

**Table 3.1:** Initial conditions - Fitted Parameters

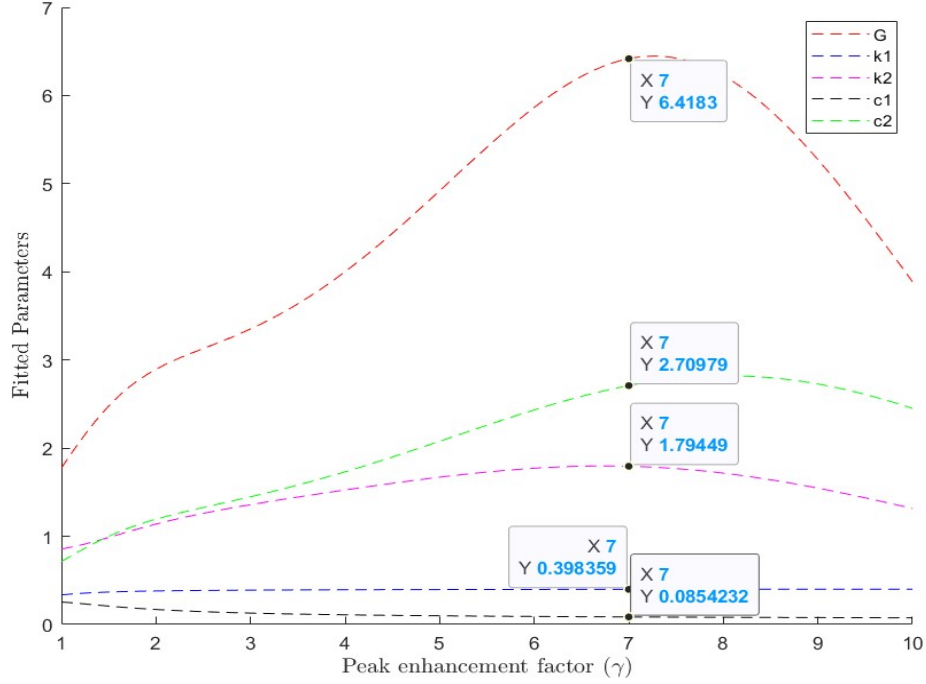


**Figure 3.2:** Fitting parameter vs Peak Enhancement factor ( $\gamma$ )

Taking into account the above considerations, a well approximated spectrum is deduced. It is important to remark that the JONSWAP spectrum shape parameters to obtain the following spectrum are  $H_s = 1, \gamma = 2$  and  $T_p = 10$  (Fig.3.4).

### 3.3 Response of the System to Random Inputs

In order to obtain a power spectrum close to the JONSWAP spectrum, it was done an excitation by unit-intensity i.e  $S_{(w)} = |F_w(jw)|^2$ .

#### 3.3.1 State- Space Modelling

The model used is based on a cascade of two second order filters (Eq.3.2). In first instance, It is needed to derived this representation from a differential second order dynamic system as follows:

Set the second order non-homogeneous differential equation (DE) for second

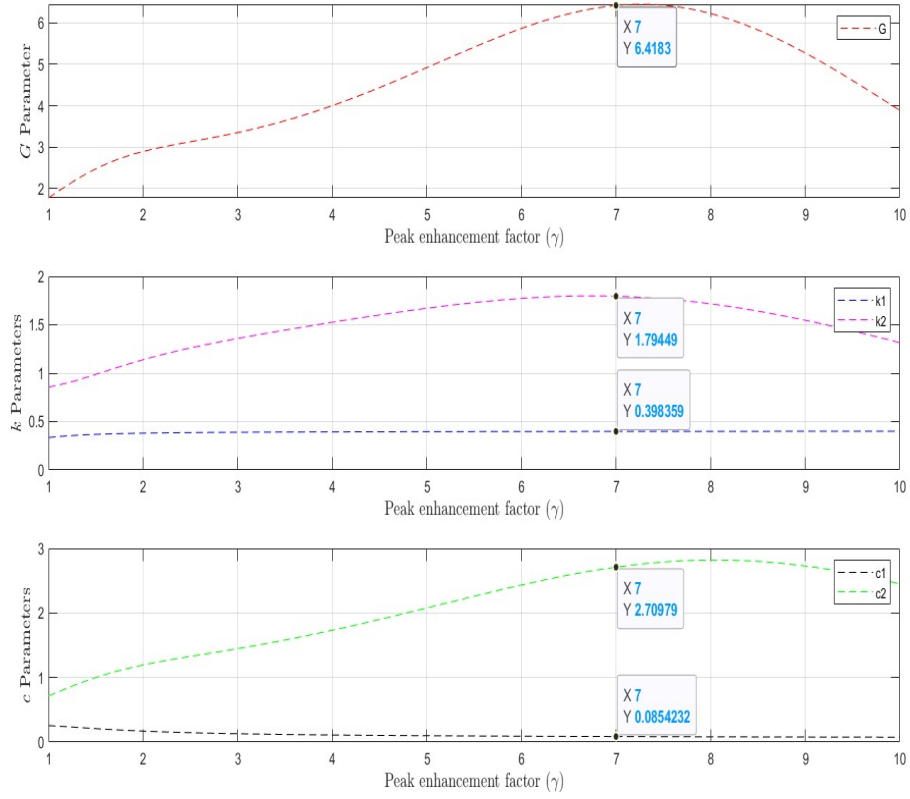


**Figure 3.3:** Fitting parameter vs Peak Enhancement factor ( $\gamma$ ) - Initial conditions

order filter.

$$M\ddot{x} + C\dot{x} + Kx = f(t) \quad (3.5)$$

Solving the non-homogeneous DE. The solution will be given by  $x(t) = Xe^{wt}$ .

$$X[-Mw^2 + jwC + K] = F(t) \quad (3.6)$$

Obtaining the system response.

$$X = \frac{F(t)}{(K - Mw^2) + jwC} \quad (3.7)$$

In order to acquire the needed gain ( $g$ ) is now need to factor out the inertial constant  $M$ .

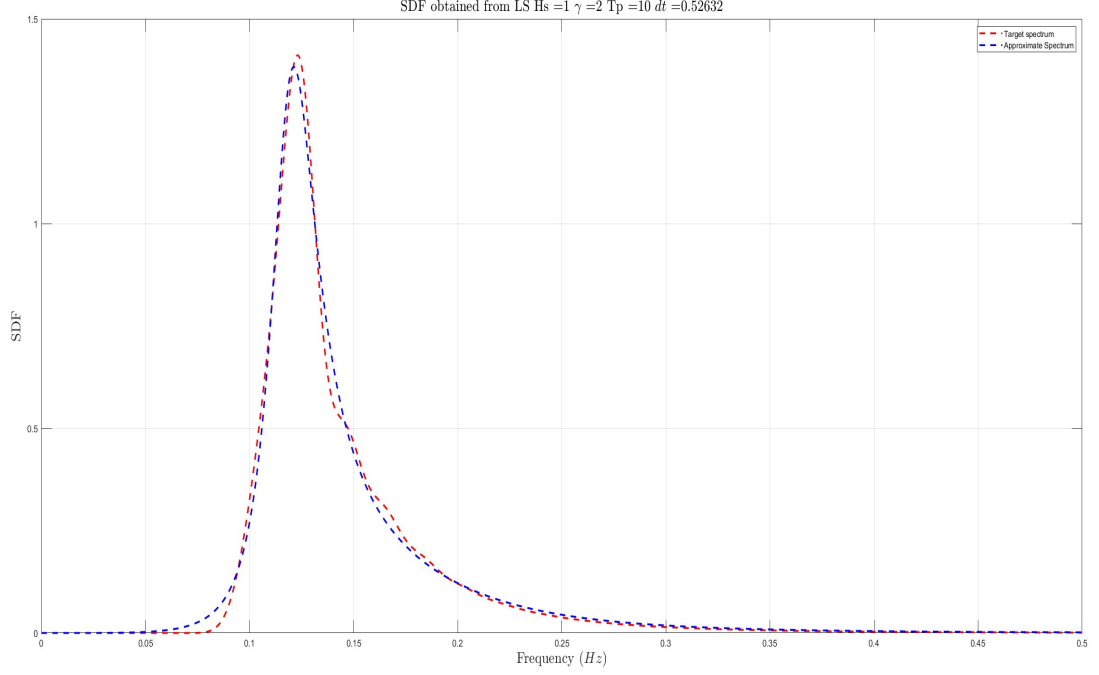


**Figure 3.4:** Spectral density function - Target spectrum and Approximate spectrum  $H_s = 1, \gamma = 2$  and  $T_p = 10$

$$X = \frac{\frac{F(t)}{M}}{(k - w^2) + jwc} \quad (3.8)$$

Finally, to have the form a of a second order filter is needed to multiply by  $\frac{K}{K}$ . And remembering that  $\frac{K}{M} = w^2$

$$X = \frac{\frac{F(t)w^2}{K}}{(k - w^2) + jwc} \quad (3.9)$$

Be  $g = \frac{F(t)}{K}$

$$X = \frac{gw^2}{(k - w^2) + jwc} \quad (3.10)$$

From Eq. 3.5 is now implemented the following differential equations in order to create the State-Space model.

$$\ddot{x}_1 + c_1\dot{x}_1 + k_1x_1 = g_1 \quad (3.11)$$

$$\ddot{x}_2 + c_2\dot{x}_2 + k_2x_2 = g_2 \quad (3.12)$$

Once this representation is set, it is necessary to transform it in a State-space model form. Starting from the first second order filter.

$$\begin{bmatrix} \dot{x}_1 \\ \ddot{x}_1 \end{bmatrix} = \begin{bmatrix} 0 & 1 \\ -k_1 & -c_1 \end{bmatrix} \begin{bmatrix} x_1 \\ \dot{x}_1 \end{bmatrix} + \begin{bmatrix} 0 \\ 1 \end{bmatrix} g_1 \quad (3.13)$$

Note that the measurable output which allows to understand the dynamics is the variable  $\dot{x}_1$ .

$$y_1 = \begin{bmatrix} 0 & 1 \end{bmatrix} \begin{bmatrix} x_1 \\ \dot{x}_1 \end{bmatrix} \quad (3.14)$$

Following the same procedure above the second State-space model will be set as:

$$\begin{bmatrix} \dot{x}_2 \\ \ddot{x}_2 \end{bmatrix} = \begin{bmatrix} 0 & 1 \\ -k_2 & -c_2 \end{bmatrix} \begin{bmatrix} x_2 \\ \dot{x}_2 \end{bmatrix} + \begin{bmatrix} 0 \\ 1 \end{bmatrix} g_2 \quad (3.15)$$

The output measurable variable will be  $\dot{x}_2$ :

$$y_2 = \begin{bmatrix} 0 & 1 \end{bmatrix} \begin{bmatrix} x_2 \\ \dot{x}_2 \end{bmatrix} \quad (3.16)$$

Having these two State-space models which represents a second order filter each one. Now is necessary to have a general expression for a cascade of two State-space models as follows:

$$\begin{cases} \dot{x}_1 = A_1 x_1 + B_1 u_1 \\ y_1 = C_1 x_1 + D_1 u_1 \end{cases} \quad (3.17)$$

$$\begin{cases} \dot{x}_2 = A_2 x_2 + B_2 u_2 \\ y_2 = C_2 x_2 + D_2 u_2 \end{cases} \quad (3.18)$$

Be the output  $y_1$  of the expression 3.17 is the input  $u_2$  of the expression 3.18. The expression 3.18 will be written as:

$$\begin{cases} \dot{x}_2 = A_2x_2 + B_2(C_1x_1 + D_1u_1) \\ y_2 = C_2x_2 + D_2(C_1x_1 + D_1u_1) \end{cases} \quad (3.19)$$

Be expression 3.17 in expression 3.19 is obtained the expressions 3.20. This is the compact State-Space model form needed to be implemented:

$$\begin{cases} \dot{x}_1 = A_1x_1 + B_1u_1 \\ \dot{x}_2 = A_2x_2 + B_2C_1x_1 + B_2D_1u_1 \\ y_2 = C_2x_2 + D_2C_1x_1 + D_2D_1u_1 \end{cases} \quad (3.20)$$

Above expression can be written in matrix form:

$$\begin{cases} \begin{bmatrix} \dot{x}_1 \\ \dot{x}_2 \end{bmatrix} = \begin{bmatrix} A_1 & 0 \\ B_2C_1 & A_2 \end{bmatrix} \begin{bmatrix} x_1 \\ x_2 \end{bmatrix} + \begin{bmatrix} B_1 \\ B_2D_1 \end{bmatrix} u_1 \\ y_2 = \begin{bmatrix} D_2C_1 & C_2 \end{bmatrix} \begin{bmatrix} x_1 \\ x_2 \end{bmatrix} + \begin{bmatrix} D_2D_1 \end{bmatrix} u_1 \end{cases} \quad (3.21)$$

Taking into account expression 3.21, Eq 3.11 and Eq 3.12, also considering the product between  $g_1g_2 = G$  The implemented State-space model is:

$$x_t = \begin{bmatrix} x_1 \\ \ddot{x}_1 \\ x_2 \\ \ddot{x}_2 \end{bmatrix} = \begin{bmatrix} \begin{bmatrix} 0 & 1 \\ -k_1 & -c_1 \end{bmatrix} & \begin{bmatrix} 0 & 0 \\ 0 & 0 \end{bmatrix} \\ \begin{bmatrix} 0 \\ 1 \end{bmatrix} & \begin{bmatrix} 0 & 1 \\ -k_2 & -c_2 \end{bmatrix} \end{bmatrix} \begin{bmatrix} x_1 \\ \dot{x}_1 \\ x_2 \\ \dot{x}_2 \end{bmatrix} + \begin{bmatrix} 0 \\ 1 \\ 0 \\ 0 \end{bmatrix} G \quad (3.22)$$

The output expression of the State-space model is:

$$y_t = \begin{bmatrix} 0 & 0 & 0 & 1 \end{bmatrix} \begin{bmatrix} x_1 \\ \dot{x}_1 \\ x_2 \\ \dot{x}_2 \end{bmatrix} \quad (3.23)$$

### 3.3.2 Stochastic signal processing

The resulting State-space model from Eq. 3.22 when excited by unit-intensity white noise, its power spectrum is close to the JONSWAP spectrum i.e  $S_{(w)} = |F_w(jw)|^2$  [20]. Every time this model is excited with random signal, the result will be called a *realization*.

At this point, to obtain the spectral properties and notice a clear pattern of JONSWAP spectrum from the realizations performed before, it was implemented averaging across different repetitions of random realizations in a time  $t$  each SDF.

When this procedure is ready, is observed an attenuation (Aliasing effect) (Fig. 3.5) of the spectrum after exciting it with the unit-intensity white noise. This is mainly due to not selecting the proper bandwidth spectrum. For this, an extreme caution must be taken for selecting the frequency bandwidth.

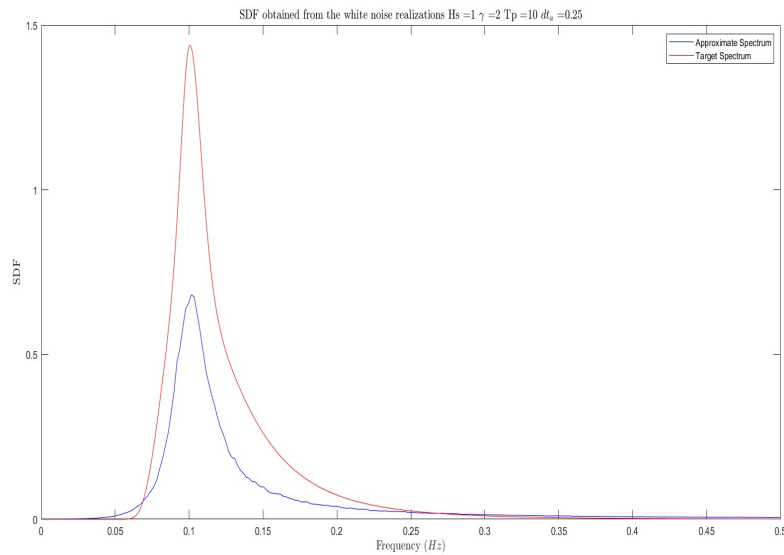


**Figure 3.5:** Spectral density function - Approximate spectrum and Target Spectrum

In real time measuring, it is not possible to know what are going to be the signals that our system will deal with. By sorting the measured signals into a specific category and delimiting the statistical properties of the class of expected inputs will contribute in a proper signal processing.

Before calculating the SDF, it is needed to analyze the State-space model's bandwidth frequency by using a frequency analysis in order to find a proper sampling time.

### 3.3.3 Bandwidth selection

To select the bandwidth signal implemented in the spectrogram based on the Short-Time Fourier Transform.

In Figure 3.6, it is observed that the frequencies along the entire duration of the random realization, the beyond  $0.95Hz$ , the color pattern is having a similar color intensity (according to the range of representation in color of the power/frequency). From this point on, it is not added any value for the analysis of the signal because there is a low amplitude. Consequently, it was decided that this is the best lower frequency limit is  $0Hz$  and the upper frequency bandwidth limit  $0.95Hz$ .

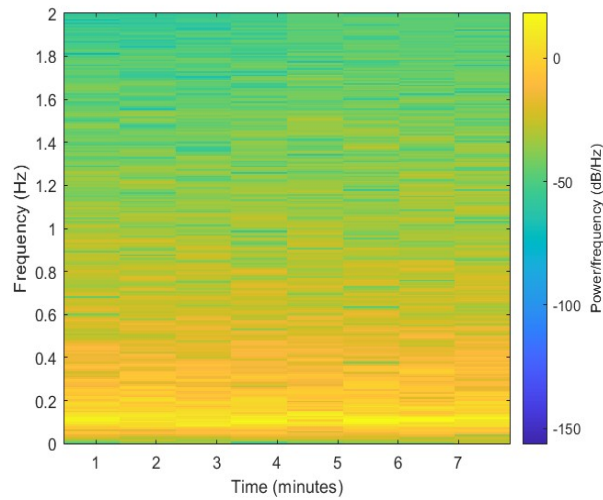


**Figure 3.6:** Spectrogram -  $\gamma = 5$   $Hz = 5$   $T_p = 10$

### 3.3.4 Low Pass Filter (LPF) Design

In real life signals are not band limited, in such cases, spectra overlapping and aliasing effects can not be avoided. The aim of applying a LPF is to prevent aliasing effect. Therefore the higher frequency components are neglected.

The anti-aliasing filter implemented is a classic IIR Butterworth. Having the bandwidth  $w_b = 0.95Hz - 0Hz$ , it enables to select the minimum sampling rate also known as nyquist frequency  $w_n = 2w_b$  and the time intervals  $T_s = 1/w_n$ . The SDF obtained with the selected bandwidth and changing the JONSWAP shape parameters are shown in Fig 3.7.

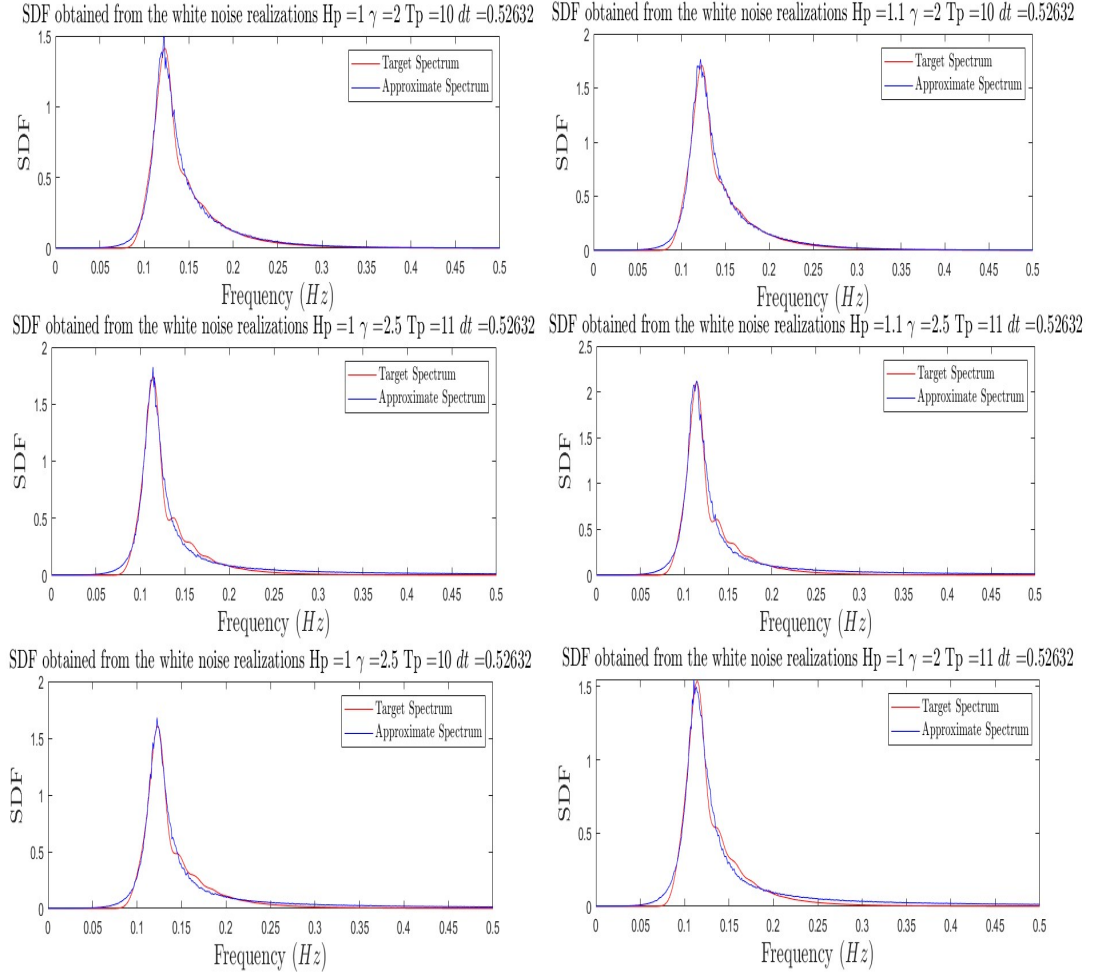


**Figure 3.7:** SDF comparison

Note that this procedure was only to introduce a JONSWAP spectrum contained in a white noise signal and having a proper state space model to develop the Kalman filter design. Considerable care must be taken when performing future simulations by taking into consideration the statistical properties and set a proper bandwidth and sensor as well.

### 3.3.5 Stability and Steady state analysis

In order to guaranty the stability in the state-space model, it is needed to set the poles in the left section of the z-plane. Taking into account the constraints in Subsection. 3.2, the values of the poles in Fig.3.8 will define a stable behaviour of the state space model.

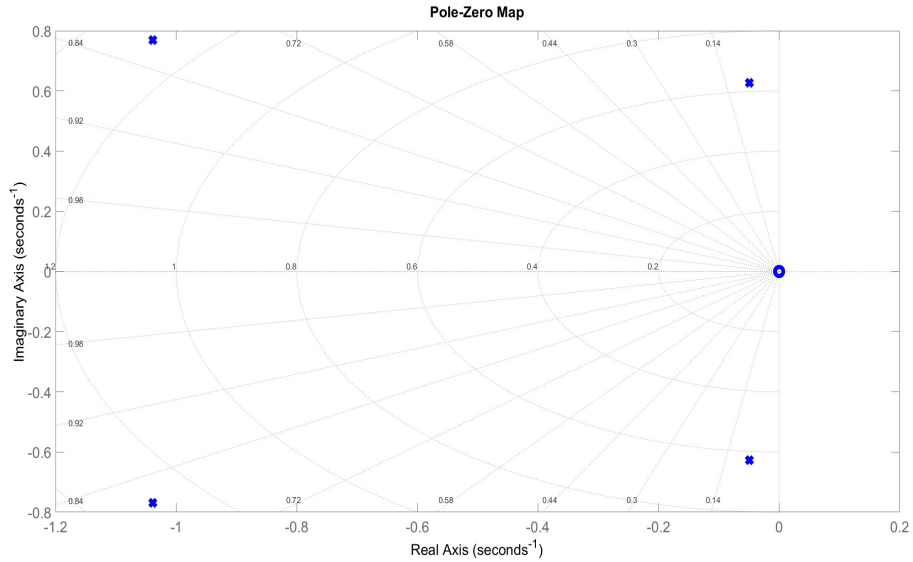


**Figure 3.8:** Zero and Poles locations

Furthermore, it was decided that the best procedure to verify its stability was to excite the State-Space model with a step signal. As can be seen in Fig. 3.9, it will result in several oscillations due to the poles locations, also its settling time (extinction quickness) will around 82.2 seconds.

## 3.4 Kalman Filter Design

The kalman filter design is considered combining the results obtained in the previously state-space model Eq. 3.22 and Eq. 3.23 which is also a discrete time linear system.

The random variables  $w_{t-1}$  and  $v_t$  based on Eq.2.25 and Eq.2.26 respectively are also independent from each other. One considered white noise process noise and the other, a normal distributed measurement noise.

$$x_t = Ax_{t-1} + Bu_{t-1} + w_{t-1} \quad (3.24)$$

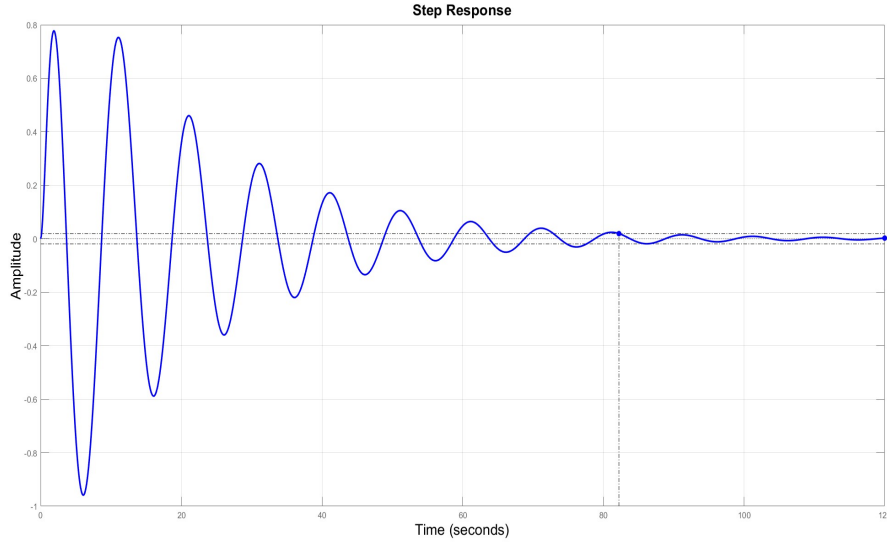


**Figure 3.9:** Step response

$$y_t = Cx_t + v_t \quad (3.25)$$

The design of the Extended Kalman Filter was also based the initial conditions are  $x_o = [0 \ 0 \ 0 \ 0]^T$  and initial estimate for the covariance matrix  $P_o = BQB^T$  and be  $Q = 1$  (white noise). Also any input signal  $u_{t-1}$  be considered.

### 3.4.1 Prediction step

In every time step  $t$  of the system its propagated the estimate forward in time according to the dynamics of state-space model. Great care must be taken, because in Eq.3.26 the term  $w_{t-1}$  stated in Eq. 3.24 do not appear due to it has zero mean (white noise).

$$\hat{x}_t^- = g(u_t, x_{t-1}) \quad (3.26)$$

The covariance (uncertainty of the estimate), in literature also known as A priori error covariance is propagated forward in time. The A priori estimate error  $e_t^- = x_t - \hat{x}_t^-$  in the discrete time system evolves as,  $e_t^- = Ae_{t-1}^- + w_t$  and applying Eq.2.11 is obtained Eq.3.27

$$P_t^- = AP_{t-1}A^T + Q \quad (3.27)$$

### 3.4.2 Correction Step

Once a measurement from any JONSWAP spectrum is given to the kalman filter, the gain matrix  $K_t$  is computed in Eq. 3.28. Note that  $R = E[vv^T]$  represent the covariance matrix of the normal distributed measurement noise  $v_t$  :

$$K_t = P_t^- C^T (C P_t^- C^T + R)^{-1} \quad (3.28)$$

This Eq. 3.28 is use to update its precedent estimate state  $\hat{x}_t$  (Eq. 3.29) and the A posteriori error covariance (Eq. 3.30):

$$\hat{x}_t = \hat{x}_t^- + K_t(y_t - h(\hat{v}_t^-)) \quad (3.29)$$

$$P_t = (I - K_t C) P_t^- \quad (3.30)$$

### 3.4.3 Block diagram scheme

The plan model in Fig.3.10, is excited with a the process noise  $w$  (unity intensity white-noise signal), this is the only input for the kalman filter is the plant model with a measurement noise added. It will not be considered any other input. Next, this plant model passes through the LPF preventing any aliasing effect. Consecutively, is performed the discretization of the system ( $A/D$ ), because the kalman filter has been modeled in the continuous time-domain.

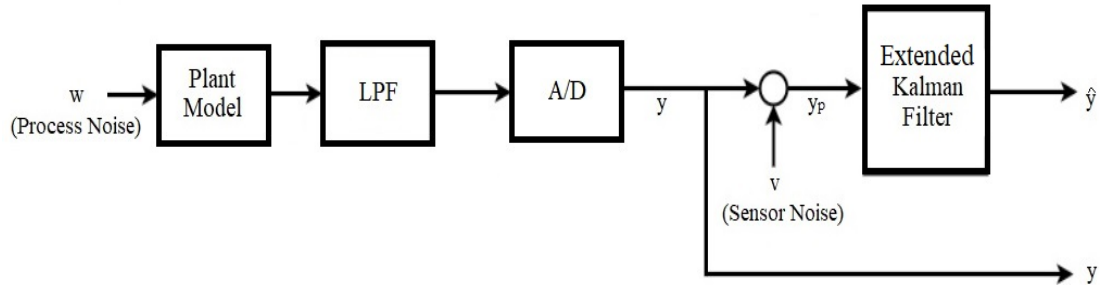


**Figure 3.10:** Block diagram Scheme

In addition, the sensor noise has been considered with a low covariance as possible, assuming the measurement are not going to be disrupted in a big manner.

These are the signals on the scheme:

- $w$  - Unity intensity white-noise signal.

- $y$  - Output of the plan model (P-M) after the discretization.
- $y_p$  - Output of the plan model (P-M) after adding the measurement noise.
- $\hat{y}$  - Estimated output from the kalman filter.

# Chapter 4

## Results and Discussion

### 4.1 Calculation Procedure Setup

#### 4.1.1 Equivalent conditions

The general aspects for the kalman filter are already performed, from now on the state-space model used to design its behaviour is named as "nominal model" (N-M). It is important to remark that this model have been optimized according to the Least-Squares Spectral approximation (Ch.3.1) and assumed JONSWAP spectrum shape parameters (Table 4.1).

Hs	$\gamma$	$T_p$
1	2	10

**Table 4.1:** Assumed spectrum parameters - Nominal model

Firstly, in order to analyse the behaviour of the kalman filter is considered a plant model (P-M) which generates random realization signal as an input to the Extended Kalman Filter with the same assumed JONSWAP spectrum shape parameters (Table 4.1).

In Fig 4.1, is observed that the kalman random realization is almost equal to the P-M random realization. This is also evident after performing the estimation error calculation between these two signals i.e  $|Target - Estimated| = 0.0055473$ . Also by setting the confidence intervals can be deducted that at 95% confidence level the prediction error (Kalman Filter-Estimated) will be within.

Subsequently, it is calculated the SDF for each realization after averaging them across 10.000 different repetitions for each time  $t$  (Fig.4.2), obtaining a quite narrow

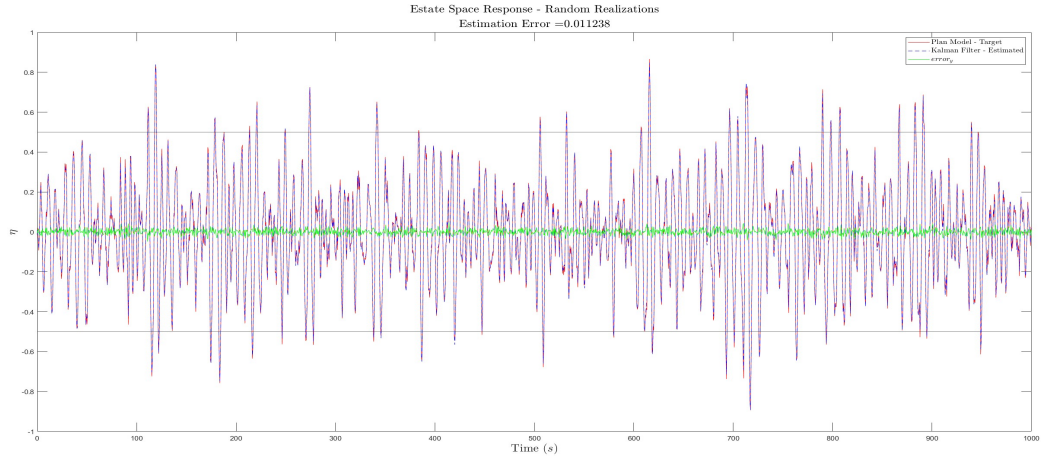


**Figure 4.1:** Target and Estimated realizations - Equivalent conditions

estimation of the P-M target spectrum.

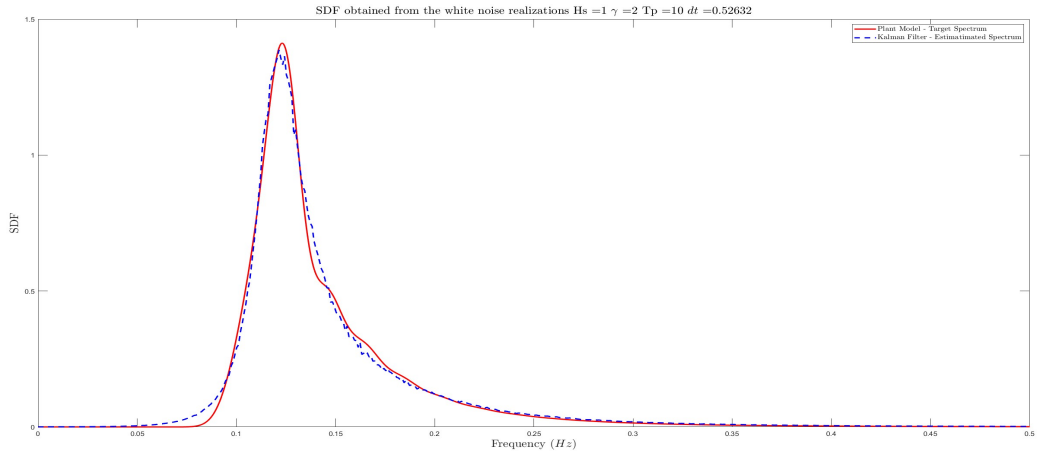


**Figure 4.2:** P-M Target Spectrum, Kalman filter - Estimated Spectrum - Equivalent conditions

In the other hand, the only state variable ( $x_2$ ) that is controlled in the output of the state space model (Eq.3.23) will behave within the confidence intervals (confidence level 95%) as expected from a normal distribution and the error  $|Target - Estimated| = 0.094848$  (Fig.4.3).

Finally, the observed estimating behaviour of the kalman filter in equal condition with respect to the plan model is clearly well approximated. This test reveals the

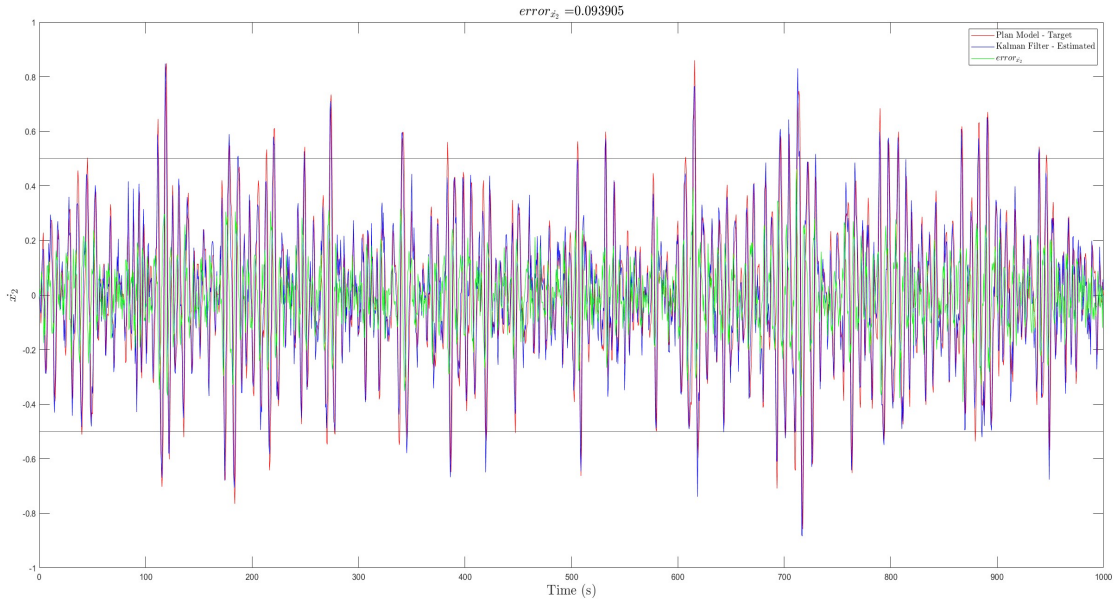


**Figure 4.3:** State Variable  $x_2$  - Equivalent conditions

accurate behaviour that the EKF is presenting. As forecast, this analysis prove the excellent performance using the EKF to estimate the JONSWAP spectrum, although in the following subsections the random conditions are going to be considered.

#### 4.1.2 Different conditions

**Hs = 1.1,  $\gamma=2$ , Tp=10**

In Fig.4.7.a, is observed the estimation error between these two signals (output response) i.e  $|Target - Estimated| = 0.011478$ . Apart from the slight non-alignment by setting the confidence intervals, the result is confirmation of the prediction error (Kalman Filter- Estimated) will be within at least the 95% of the runs of the random realizations.

Its SDF for each realization averaged across 10.000 different repetitions for each time  $t$  (Fig.4.7.b), the estimated JONSWAP spectrum is quite close to the P-M target spectrum, as expected based on Fig.4.7.a.

The state variable ( $x_2$ ) will behave within the confidence intervals (confidence level 95%) as expected from a normal distribution and the error  $|Target -$

$|Estimated| = 0.099882$  (Fig.4.7.c).

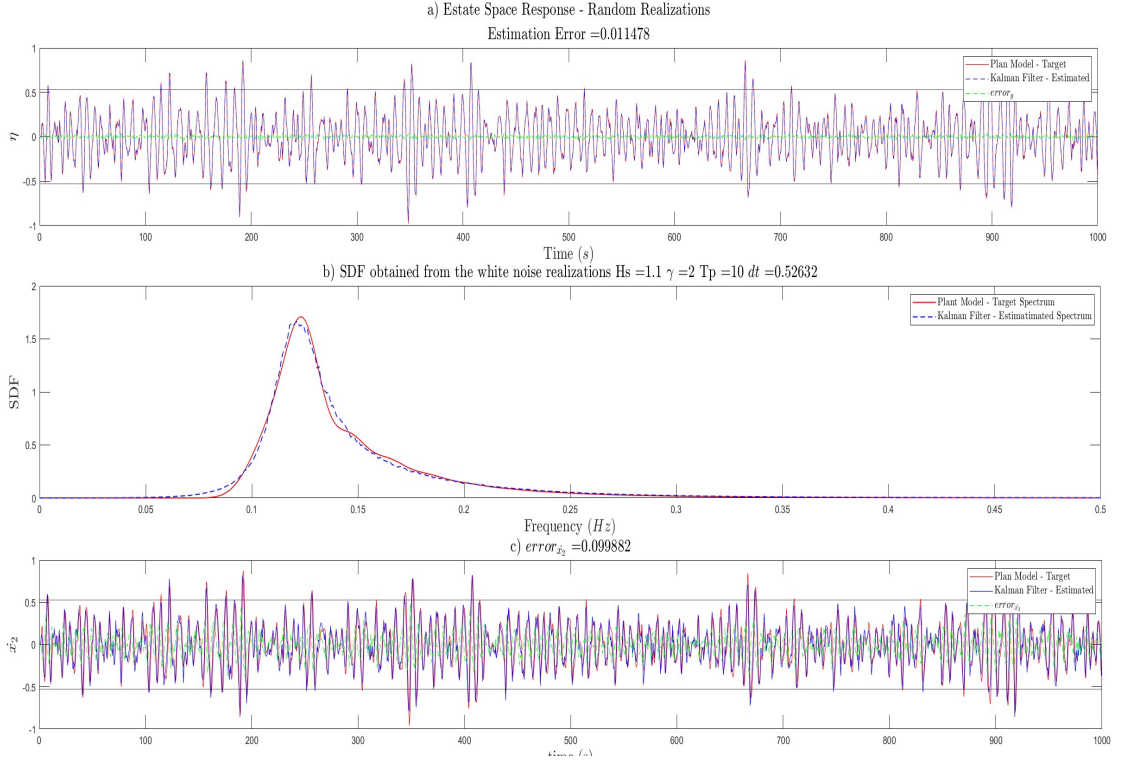


**Figure 4.4:** a) Target and Estimated realizations b) Spectrum c) State Variable  $x_2$  - P-M conditions  $H_s = 1.1, \gamma=2, T_p=10$

### $H_s = 1, \gamma=2,5 T_p=11$

In Fig.4.5.a, is observed the estimation error between these two signals (output response) i.e.  $|Target - Estimated| = 0.023377$ . Also by setting the confidence intervals, the 95% of the runs of the random realizations are within.

Despite of the non- alignment of the estimated JONSWAP spectrum (Fig.4.5.b), the findings appear to be close to the P-M target spectrum, as expected based on Fig.4.5.a.

The state variable ( $x_2$ ) will behave within the confidence intervals (confidence level 95%) as expected from a normal distribution and the error  $|Target - Estimated| = 0.10594$  (Fig.4.5.c).

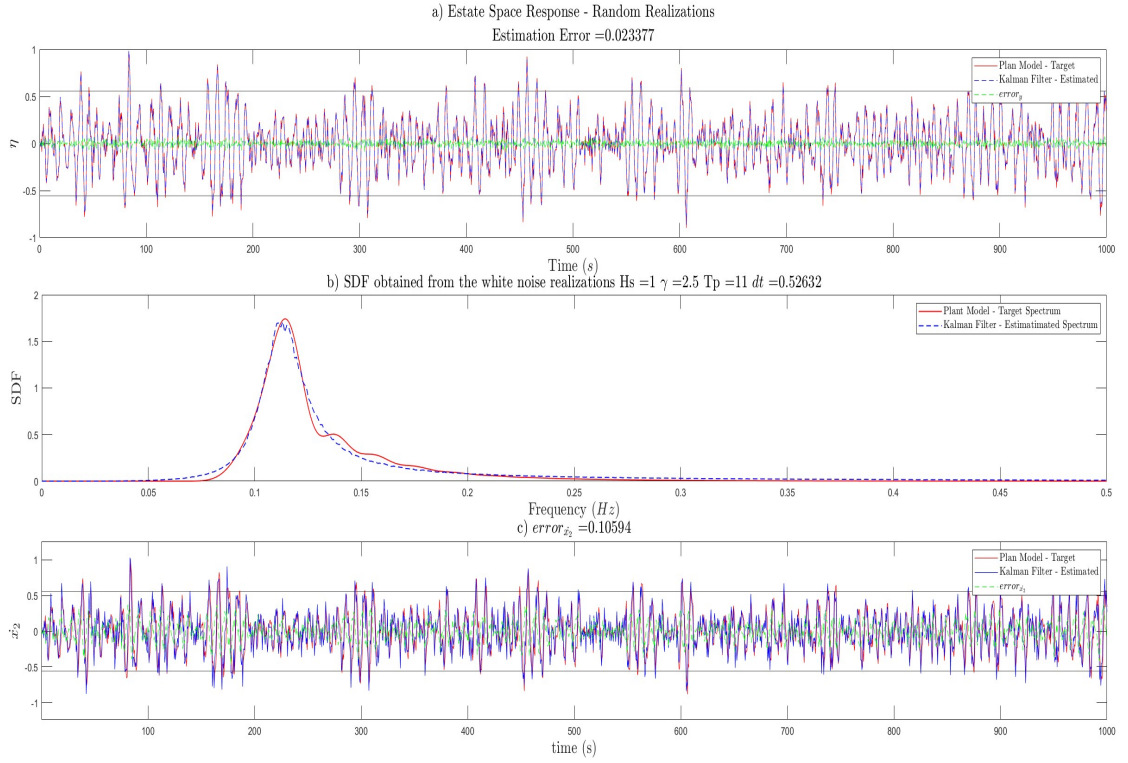


**Figure 4.5:** a)Target and Estimated realizations b)Spectrum c)State Variable  $x_2$  - P-M conditions Hs = 1,  $\gamma$ =2,5 Tp=11

### Hs = 1.1, $\gamma$ =2,5 Tp=11

It is observed in Fig.4.6, the estimation error between these two signals (output response) i.e  $|Target - Estimated| = 0.024497$ . Notwithstanding the non-alignment between the trends, by setting the confidence intervals, the prediction error (Kalman Filter- Estimated) will be within at least the 95% of the runs of the random realizations.

Its SDF for each realization averaged across 10.000 different repetitions for each time  $t$  (Fig.4.6.b), the estimated JONSWAP spectrum is quite close to the P-M target spectrum, as expected based on Fig.4.6.a.

The state variable ( $x_2$ ) has a significant behaviour behave within the confidence intervals (confidence level 95%) as expected from a normal distribution and the error  $|Target - Estimated| = 0.10537$  (Fig.4.6.c).

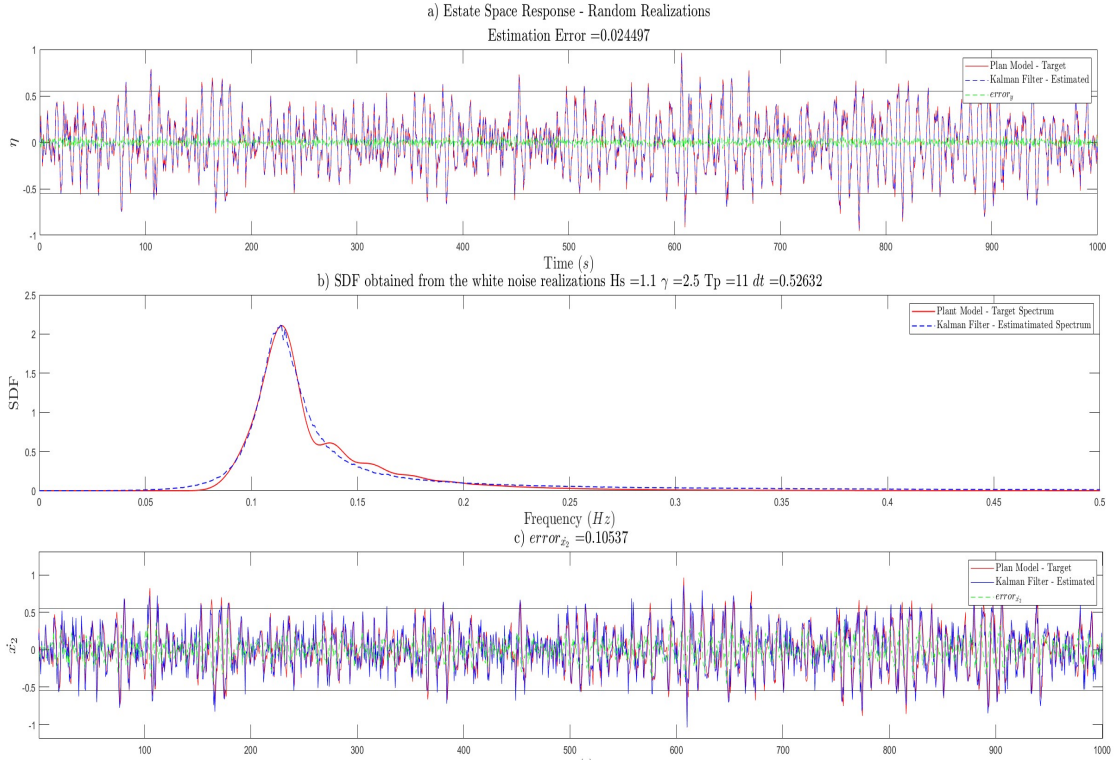


**Figure 4.6:** a) Target and Estimated realizations b) Spectrum c) State Variable  $x_2$  - P-M conditions  $H_s = 1.1$ ,  $\gamma = 2.5$   $T_p = 11$

### $H_s = 1$ , $\gamma = 2.5$ $T_p = 10$

In Fig.4.6.a, is observed the estimation error between these two signals (output response) i.e.  $|Target - Estimated| = 0.023554$ . Also by setting the confidence intervals, the prediction error (Kalman Filter- Estimated) will be within at least the 95% of the runs of the random realizations.

For each realization the SDF averaged across 10.000 different repetitions for each time  $t$  (Fig.4.6.b). Apart from this slight discordance, the result confirms that the estimated JONSWAP spectrum is quite close to the P-M target spectrum, as expected based on Fig.4.6.a.

The state variable ( $x_2$ ) will behave within the confidence intervals (confidence level 95%) as expected from a normal distribution and the error  $|Target - Estimated| = 0.1002$  (Fig.4.6.c).

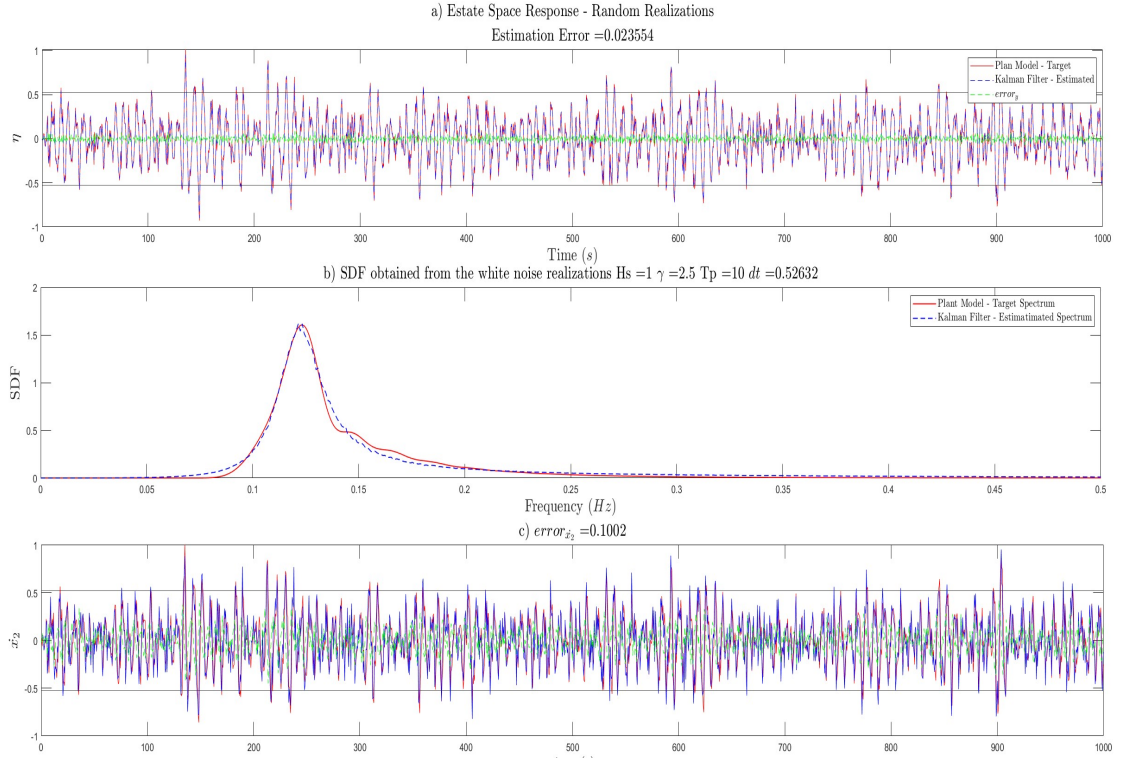


**Figure 4.7:** a) Target and Estimated realizations b) Spectrum c) State Variable  $x_2$  - P-M conditions  $H_s = 1$ ,  $\gamma=2,5$   $T_p=10$

### **$H_s = 1$ , $\gamma=2$ $T_p=11$**

In Fig.4.8.a, is observed the estimation error between these two signals (output response) i.e  $|Target - Estimated| = 0.023188$ . Also by setting the confidence intervals, the prediction error (Kalman Filter- Estimated) will be within at least the 95% of the runs of the random realizations.

Across 10.000 different repetitions for each realization averaged, its SDF for each time  $t$  (Fig.4.8.b), the estimated JONSWAP spectrum is quite close to the P-M target spectrum, as expected based on Fig.4.8.a.

The state variable ( $x_2$ ) will behave within the confidence intervals (confidence level 95%) as expected from a normal distribution and the error  $|Target - Estimated| = 0.10703$  (Fig.4.8.c).

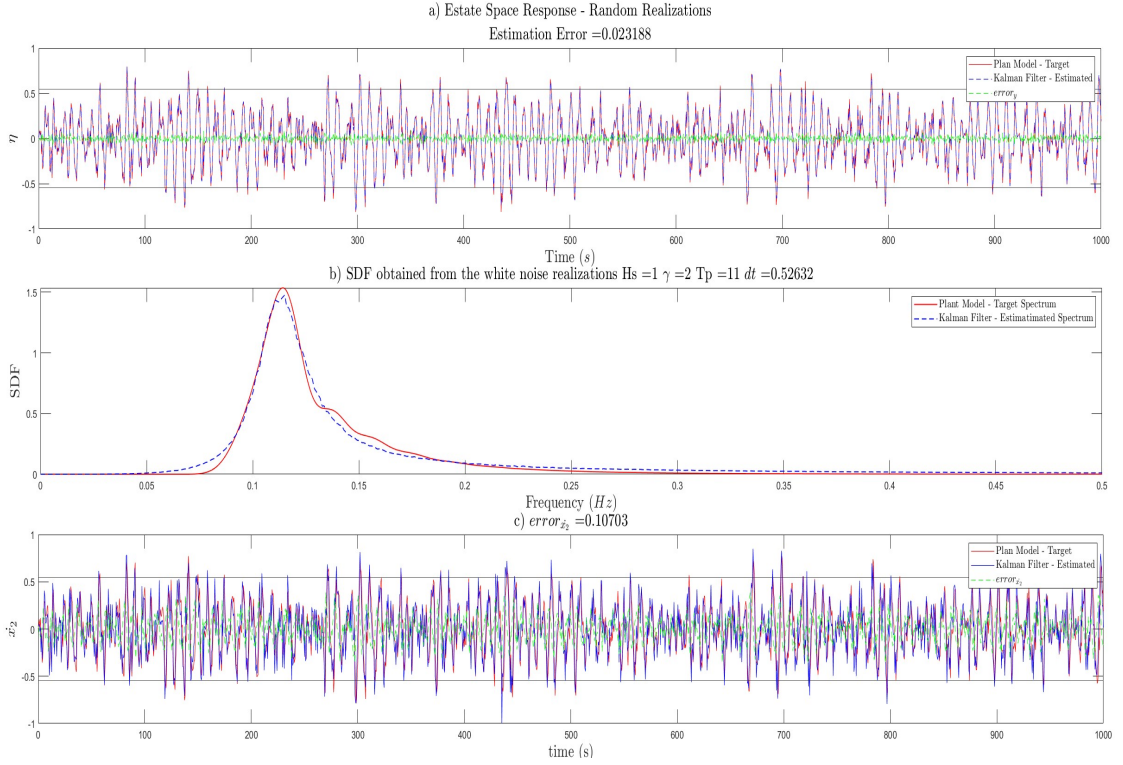


**Figure 4.8:** a)Target and Estimated realizations b)Spectrum c)State Variable  $x_2$  - P-M conditions  $H_s = 1$ ,  $\gamma=2$   $T_p=11$

### **$H_s = 2$ , $\gamma=3$ $T_p=11$**

In Fig.4.9.a, is observed the estimation error between these two signals (output response) i.e  $|Target - Estimated| = 0.018441$ . Also by setting the confidence intervals, the prediction error (Kalman Filter- Estimated) will be within at least the 95% of the runs of the random realizations.

Its SDF for each realization averaged across 10.000 different repetitions for each time  $t$  (Fig.4.9.b), the estimated JONSWAP spectrum is quite close to the P-M target spectrum, as expected based on Fig.4.9.a.

The state variable ( $x_2$ ) will behave within the confidence intervals (confidence level 95%) as expected from a normal distribution and the error  $|Target - Estimated| = 0.18681$  (Fig.4.9.c).

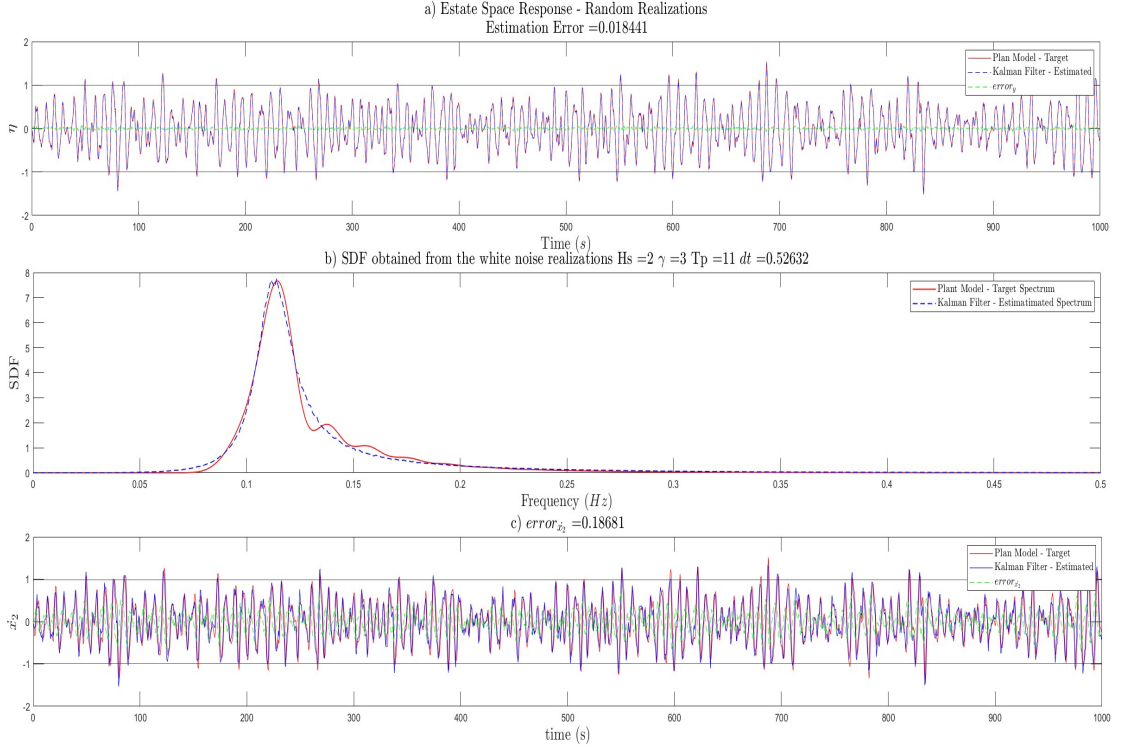


**Figure 4.9:** a)Target and Estimated realizations b)Spectrum c)State Variable  $x_2$  - P-M conditions Hs = 2,  $\gamma$ =3 Tp=11

### Hs = 3 $\gamma$ =3.3 Tp=12

In Fig.4.10.a, is observed the estimation error between these two signals (output response) i.e  $|Target - Estimated| = 0.029165$ . Also by setting the confidence intervals, the prediction error (Kalman Filter- Estimated) will be within at least the 95% of the runs of the random realizations.

Its SDF for each realization averaged across 10.000 different repetitions for each time  $t$  (Fig.4.10.b), the estimated JONSWAP spectrum is quite close to the P-M target spectrum, as expected based on Fig.4.10.a.

The state variable ( $x_2$ ) will behave within the confidence intervals (confidence level 95%) as expected from a normal distribution and the error  $|Target - Estimated| = 0.2619$  (Fig.4.10.c).

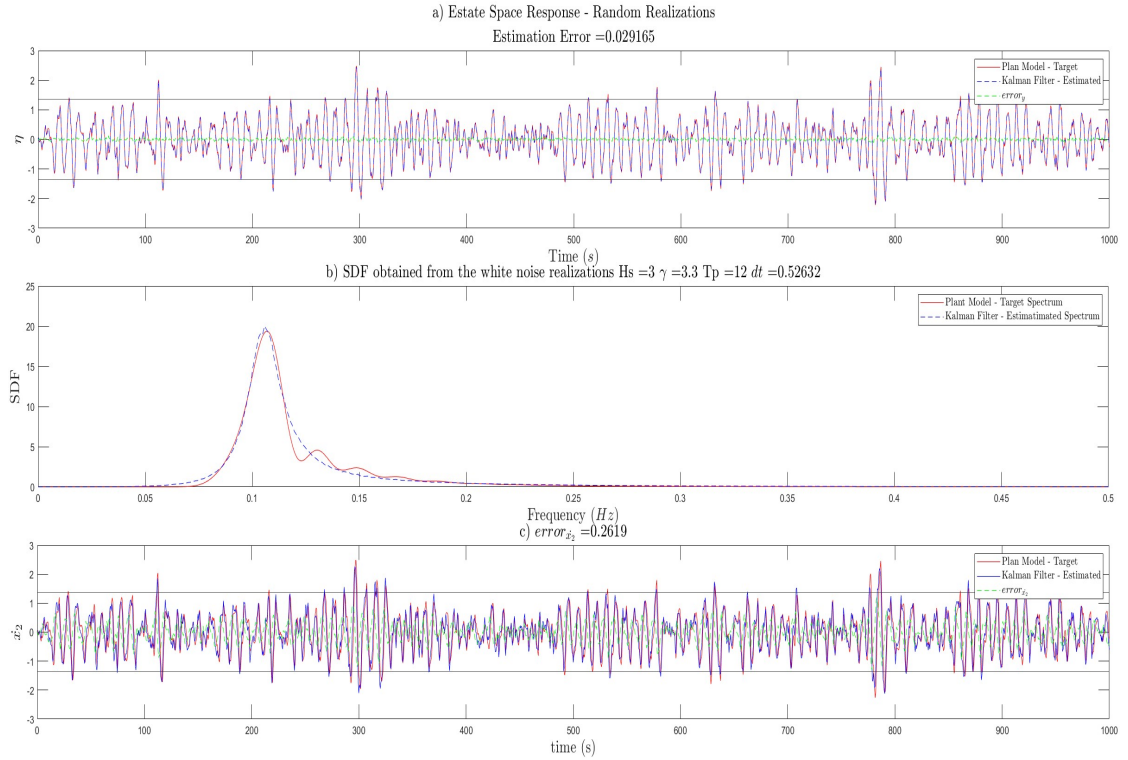


**Figure 4.10:** a)Target and Estimated realizations b)Spectrum c)State Variable  $x_2$  - P-M conditions  $H_s = 3$   $\gamma=3.3$   $T_p=12$

**$H_s = 1$   $\gamma=3$   $T_p=10$**

In Fig.4.11.a, is observed the estimation error between these two signals (output response) i.e  $|Target - Estimated| = 0.021647$ . Also by setting the confidence intervals, the prediction error (Kalman Filter- Estimated) will be within at least the 95% of the runs of the random realizations.

Its SDF for each realization averaged across 10.000 different repetitions for each time  $t$  (Fig.4.11.b), the estimated JONSWAP spectrum is quite close to the P-M target spectrum, as expected based on Fig.4.11.a.

The state variable ( $x_2$ ) will behave within the confidence intervals (confidence level 95%) as expected from a normal distribution and the error  $|Target - Estimated| = 0.10507$  (Fig.4.11.c).

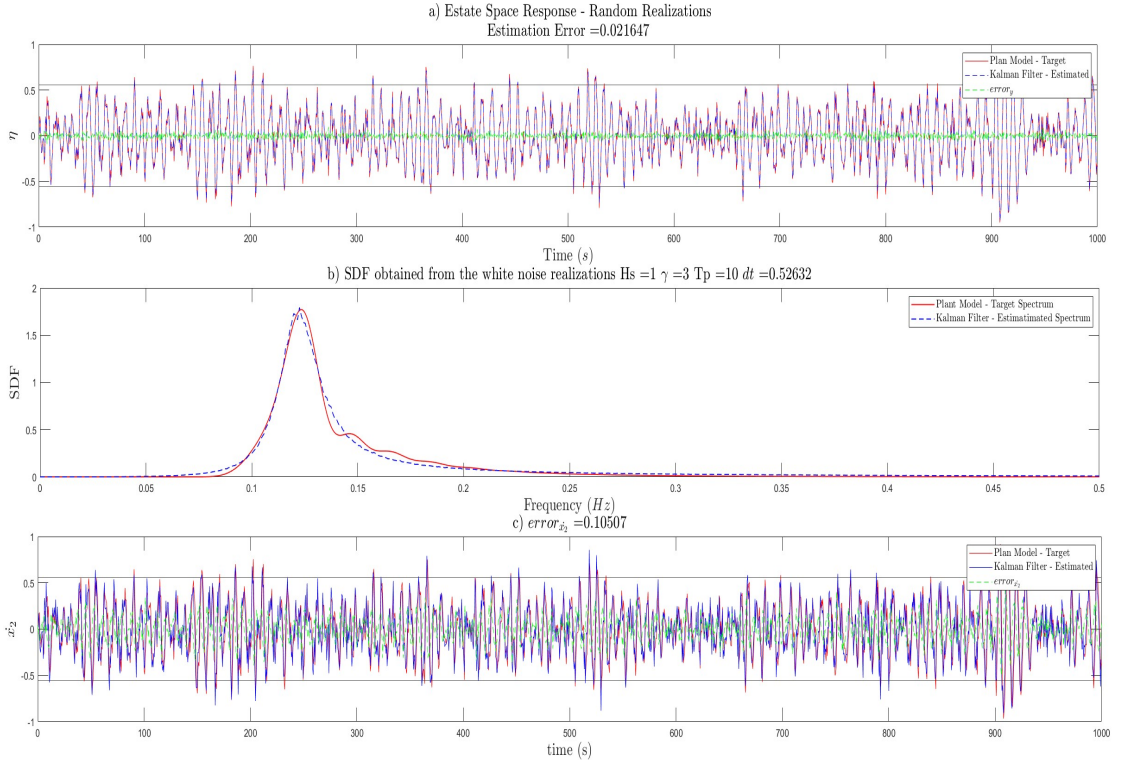


**Figure 4.11:** a) Target and Estimated realizations b) Spectrum c) State Variable  $x_2$  - P-M conditions  $H_s = 1 \gamma = 3 T_p = 10$

### $H_s = 3 \gamma = 2 T_p = 10$

In Fig.4.12.a, is observed the estimation error between these two signals (output response) i.e  $|Target - Estimated| = 0.024996$ . Also by setting the confidence intervals, the prediction error (Kalman Filter- Estimated) will be within at least the 95% of the runs of the random realizations.

Its SDF for each realization averaged across 10.000 different repetitions for each time  $t$  (Fig.4.12.b), the estimated JONSWAP spectrum is quite close to the P-M target spectrum, as expected based on Fig.4.12.a.

The state variable ( $x_2$ ) will behave within the confidence intervals (confidence level 95%) as expected from a normal distribution and the error  $|Target - Estimated| = 0.27898$  (Fig.4.12.c).

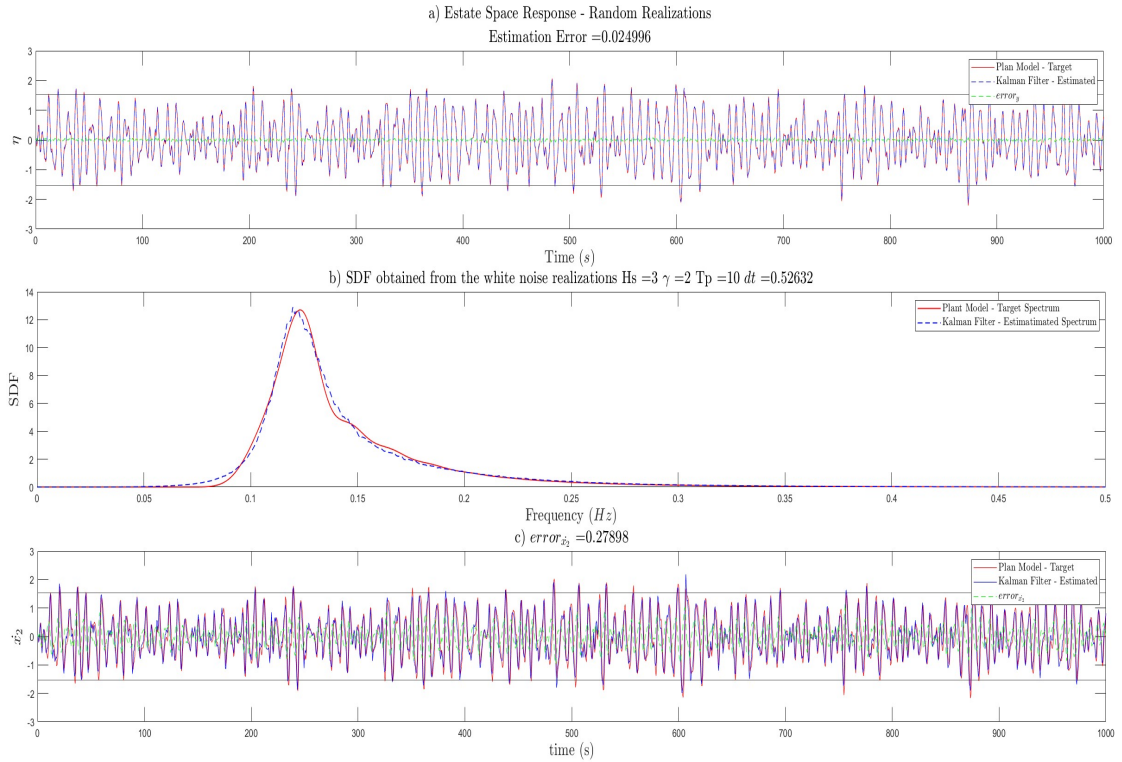


**Figure 4.12:** a)Target and Estimated realizations b)Spectrum c)State Variable  $x_2$  - P-M conditions  $H_s = 3 \gamma = 2 T_p = 10$

### $H_s = 1 \gamma = 2 T_p = 12$

In Fig.4.13.a, is observed the estimation error between these two signals (output response) i.e  $|Target - Estimated| = 0.023896$ . Also by setting the confidence intervals, the prediction error (Kalman Filter- Estimated) will be within at least the 95% of the runs of the random realizations.

Its SDF for each realization averaged across 10.000 different repetitions for each time  $t$  (Fig.4.13.b), the estimated JONSWAP spectrum is quite close to the P-M target spectrum, as expected based on Fig.4.13.a.

The state variable ( $x_2$ ) will behave within the confidence intervals (confidence level 95%) as expected from a normal distribution and the error  $|Target - Estimated| = 0.11687$  (Fig.4.13.c).

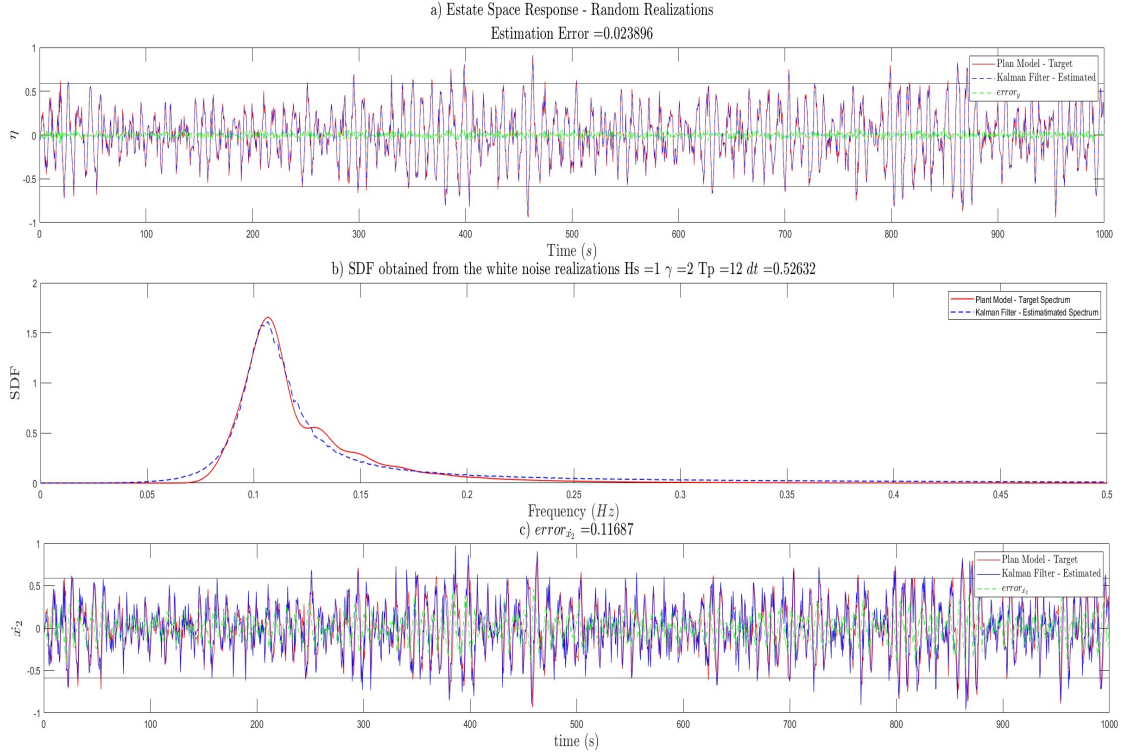


**Figure 4.13:** a)Target and Estimated realizations b)Spectrum c)State Variable  $x_2$  - P-M conditions  $H_s = 1$   $\gamma=2$   $T_p=12$

### 4.1.3 MSE analysis - Varying JONSWAP shape parameters in plant model (P-M)

To have a wide view of the kalman filter estimation behaviour, it is needed to understand how the prediction error ( $y_t - h(\hat{v}_t^-)$ ) will change while differing JONSWAP shape parameters from the P-M with respect to the nominal model (N-M).

The values obtained for  $H_s$  in Fig. 4.14 (significant wave height) varies between 0.7 to 2. It is observed that its maximum MSE at 0.00267 and its minimum value MSE at 0.0001825. At this minimum value correlates favorably well coinciding with the  $H_s = 1$  at the plan model (P-M). This confirms well that the MSE must be the minimum value when the conditions with respect the N-M and P-M are similar.

The  $T_p$  (peak wave period) in Fig. 4.15 varies between 4 to 12. Interestingly, it has found that its maximum MSE at 0.00133 and its minimum value MSE at 0.0001979 approximates to  $T_p = 10$  and this last value has a significant correlation between P-M and N-M at identical conditions.

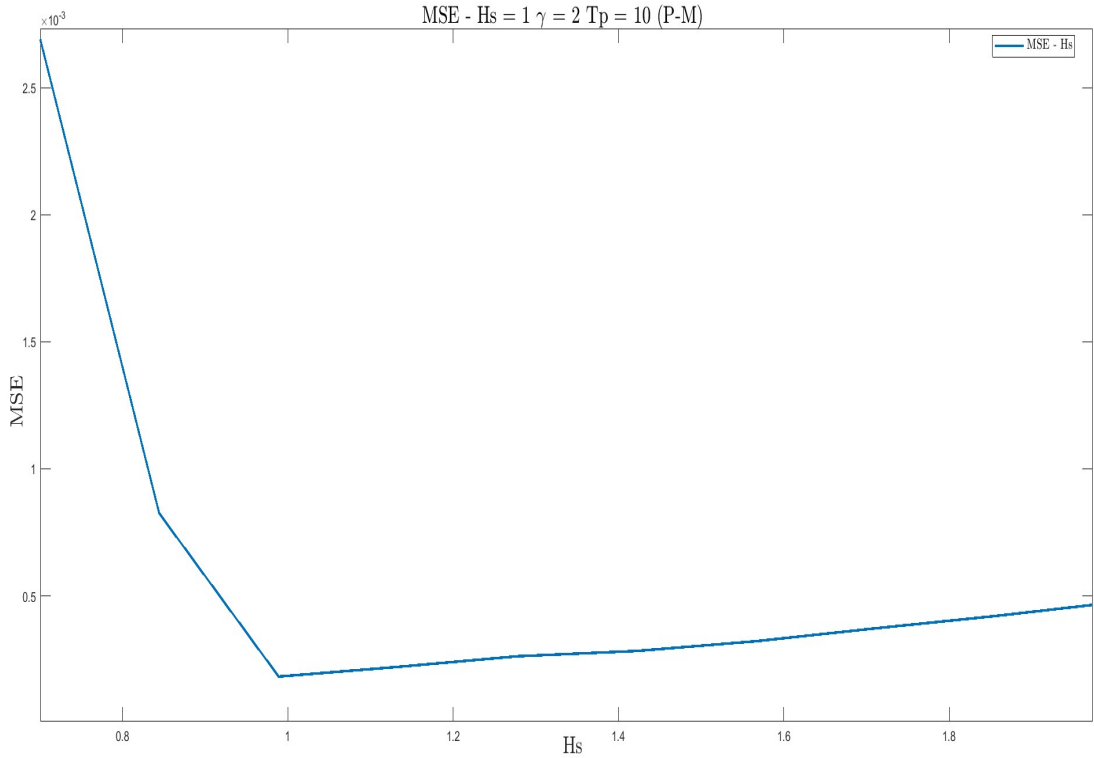


**Figure 4.14:** MSE - Varying Hs

The  $\gamma$  in Fig. 4.16 varies between 1.5 to 2.5. It is observed that its maximum MSE at 0.001055 and its minimum value MSE approximates to 0.00018307. This minimum is used to confirm when  $\gamma = 2$  is because not only N-M but also P-M are in the same  $\gamma$  conditions.

## 4.2 Results Comparison

### 4.2.1 Analysis at different conditions

In Table.4.2 are gathered all the different test performed assuming the N-M with the spectrum parameters in Table.4.1 and varying the P-M as observed in Sub-Section.4.1.2. It can be deduced, a clearly good approximations in the estimations, because not only the *estimation error* but also the *error<sub>x<sub>2</sub></sub>* are too small, this means the estimated values obtained with the kalman filter are close to the output response and state value of the P-M at each test.

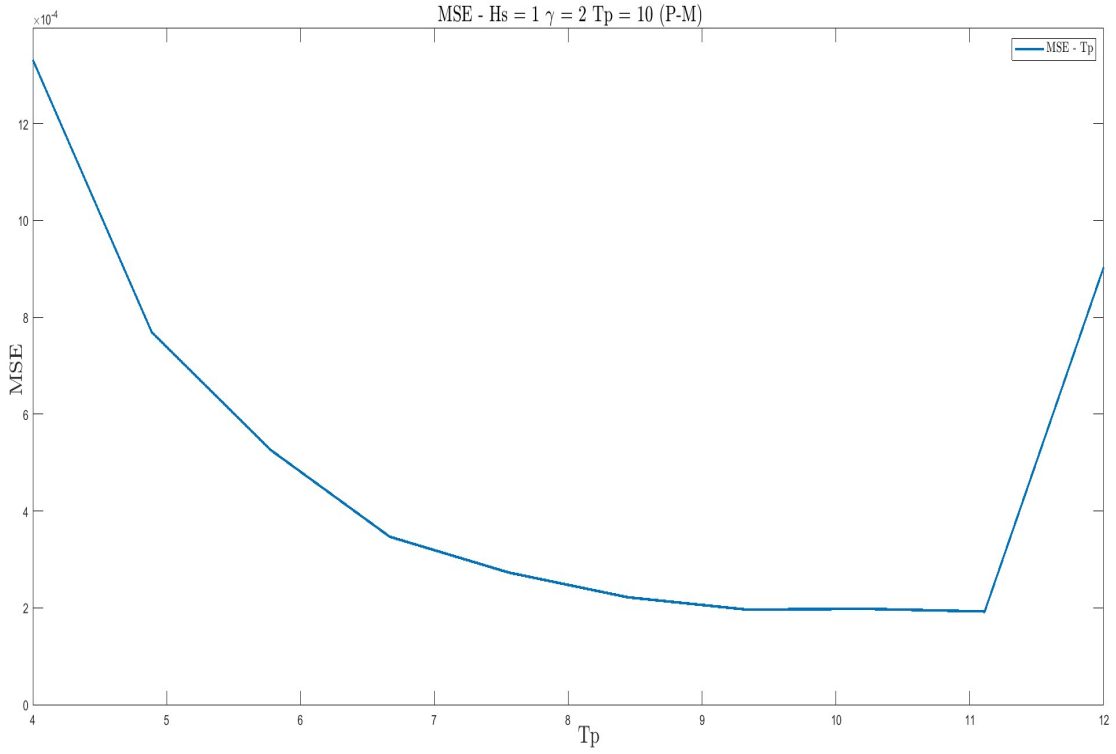
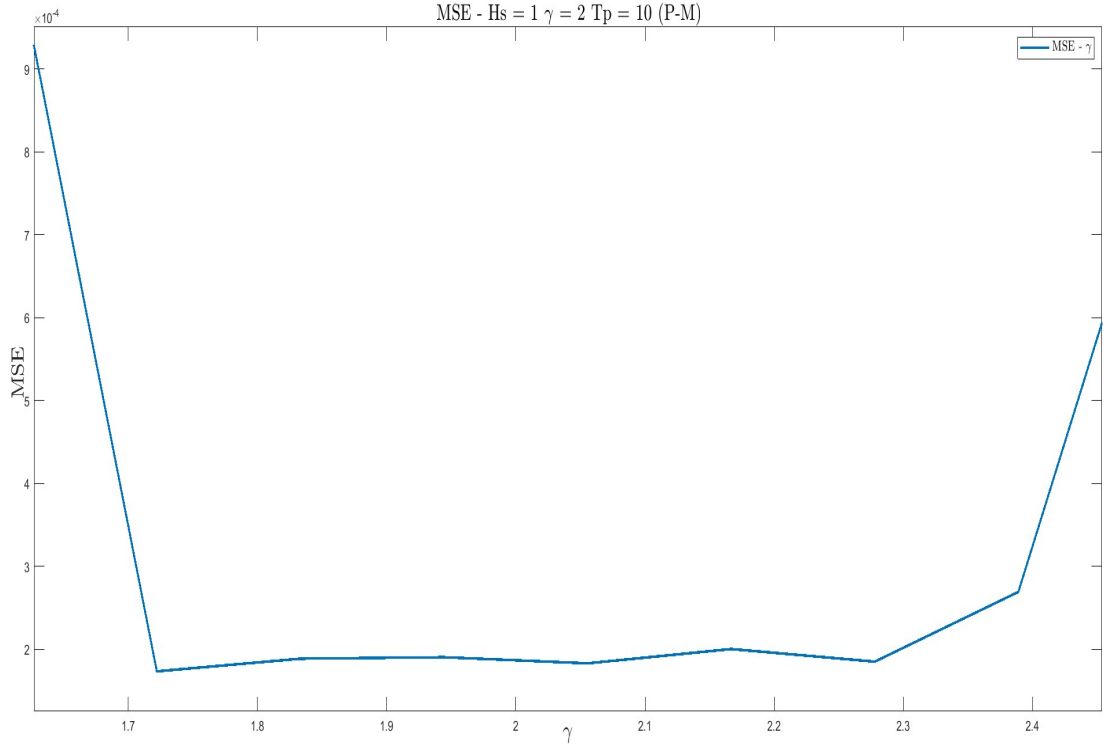


Figure 4.15: MSE - Varying Tp

N°test	Hs	$\gamma$	Tp	<i>estimation error</i>	<i>error<sub>x<sub>2</sub></sub></i>
1	1	2	10	0.011238	0.093905
2	1.1	2	10	0.011478	0.099882
3	1	2.5	10	0.023554	0.1002
4	1	2	11	0.023188	0.10703
5	3	2	10	0.024996	0.27898
6	1	3	10	0.021647	0.10507
7	1	2	12	0.023896	0.11687
8	1.1	2.5	11	0.024497	0.10537
9	1	2.5	11	0.023377	0.10594
10	2	3	11	0.018441	0.18681
11	3	3.3	12	0.029165	0.2619

Table 4.2: Different test varying the JONSWAP spectrum shape parameters with respect the N-M

As evidenced in Table. 4.2, the JONSWAP spectrum parameters that cause an increase in the *estimation error* and *error<sub>x<sub>2</sub></sub>* are the Hs (significant wave height) and



**Figure 4.16:** MSE - Varying  $\gamma$

$T_p$  (peak wave period) and  $\gamma$  (peak enhancement factor) does not have a significant weight in the variation of the prediction. Note, these results will behave in this manner only if the previously theoretical condition are accomplished.

#### 4.2.2 MSE - Analysis

The correlation in Figure.4.14, Figure.4.15 and Figure.4.16 is observed at the beginning of each figure a inversely decay in the MSE, caused by variation of each JONSWAP shape factor in the P-M. Thus, as respective JONSWAP shape factor from the P-M is getting close to the N-M which was used to design the EKF. The MSE starts to reach its minimum. This behaviour is mainly due to the EKF will generate a big positive/negative gain while it is far away from its similar condition and small positive/negative gain when the conditions are close each other.

In the other hand, once the conditions are similar or close each another, the subsequently estimations are going increase but not abruptly. Taking into consideration that MSE measures the variation with respect to the actual estimation. Note that is once again confirmed that the JONSWAP spectrum parameters that will

tend to increase the MSE are the  $H_s$  (significant wave height) and  $T_p$  (peak wave period) while  $\gamma$  (peak enhancement factor) does not have a significant increase in the MSE as it gets close to the N-M JONSWAP shape parameters.

## Chapter 5

# Conclusion and Potentially Future Work

In this research was looked to contribute with a recursive estimation of the wave spectrum by implementing an Extended-Kalman Filter.

The most marked observation to emerge from the data comparison was the performance of the EKF into the JONSWAP spectrum estimation, observing that each of the obtained realization will be desirable as realistic sea waves under this conditions. In addition the state-space model's complexity was reduced by introducing a LPF taking into account certain frequency range.

It is important to note that the comparison of the estimated spectrum obtained from the EKF with respect to the ideal JONSWAP spectrum shows a minimum MSE, meaning the estimations performed are acceptable, not only working close to the assumed (realistic) JONSWAP spectrum parameters(N-M) but also far away from them. It is important to take into consideration at any measurement a proper set of prior values, to obtain better and fast estimations.

### 5.1 Future Work

Future work need to improve the predictions of the Kalman Filter in order to establish whether is needed to take into consideration the different variations of the kalman filter for a nonlinear models as unscented kalman filter based on the EKF which performs a non-lineal transformation around a singular point or adaptive kalman filter that is based on the non-updating of the process-covariance matrix and used as initial guest for all the iteration steps.

Further studies, which take different type of sea states (a swell with narrow spectrum, a wind sea with broad spectrum and a mixed sea state with two-peak spectrum) into consideration that for each sea state, the prior initial estimates will affect in the time required for the kalman filter to obtain a proper estimation of the values.

# Appendix A

## Attestation de Stage



### ATTESTATION DE STAGE

**Organisme d'accueil : IFP ENERGIES NOUVELLES**  
1-4 AVENUE DE BOIS PREAU  
92500 RUEIL MALMAISON  
Téléphone : 01 47 52 60 00

Certifié que  
**Le stagiaire :**

**M. MONTOYA ESPINOSA DANIEL ANDRES**  
0116 CR 10B N 30A-06 PORTAL DE LA ARAUCARIAS APT 112F  
99999 SANTA ROSA DE CABAL COLOMBIE  
Mél : MUNTOIA@HOTMAIL.COM

Sexe : M Né(e) le : 22/08/1996

Etudiant(e) en : Master in Mechatronic Engineering

Au sein de (nom de l'établissement) : Politecnico di Torino

a effectué un stage prévu dans le cadre de ses études.

**Durée du stage**

Dates de début et de fin du stage : du **04/07/2022** au **16/12/2022**, soit une durée totale de stage de **5** mois et **13** jours.

**La durée du stage** est appréciée en tenant compte de la présence effective du stagiaire dans l'organisme, sous réserve des droits à congés et autorisations d'absence prévus à l'article L.124-13 du code de l'éducation (art. L.124-18 du code de l'éducation). Chaque période au moins égale à 7 heures de présence consécutives ou non est considérée comme équivalente à un jour de stage et chaque période au moins égale à 22 jours de présence consécutifs ou non est considérée comme équivalente à un mois.

Fait à RUEIL MALMAISON, le 16/12/2022



Stéphanie RENAUDIN  
Gestionnaire RH

**L'attestation de stage** est indispensable pour pouvoir, sous réserve du versement d'une cotisation, faire prendre en compte le stage dans les droits à retraite. La législation sur les retraites (loi n°2014-40 du 20 janvier 2014) couvre aux étudiants **dont le stage a été gratifié** la possibilité de faire valider celui-ci dans la **limite de deux trimestres**, sous réserve de **versement d'une cotisation**. La **demande est à faire par l'étudiant dans les deux années** suivant la fin du stage et sur **présentation obligatoire de l'attestation de stage** mentionnant la durée totale du stage et le montant total de la gratification perçue. Les informations précises sur la cotisation à verser et sur la procédure à suivre sont à demander auprès de la sécurité sociale (code de la sécurité sociale art. L.351-17 ; code de l'éducation art. D.124-9).

**IFP Energies nouvelles**  
EPIC - RCS 775 729 155 Nanterre - APE : 7219Z  
1 et 4 avenue de Bois-Préau - 92852 Rueil-Malmaison Cedex - France  
Tél : +33 1 47 52 60 00 - Fax : +33 1 47 52 70 00

[www.ifpenergiesnouvelles.fr](http://www.ifpenergiesnouvelles.fr)

Figure A.1: Attestation de Stage

## Appendix B

# Extended - Kalman Filter MATLAB code implementation

```
1 clc
2
3 close all
4
5 clear
6
7 rng('shuffle')
8
9 %% -----Defining the frequency range for the Kalman-----
10
11 df = 1e-3; % frequency step [Hz]
12
13 fc = 2; % cut-off frequency [Hz]
14
15 Tsim = 1000; % Duration of the simulated signal [s]
16
17 Bandwidth = 0.95-0; % [Hz]
18
19 dt = 1/(2*Bandwidth); % Time step
20
21 fs = 1/dt; % Frequency Step
22
23 t = 0:dt:Tsim; % Time
24
25 f = (0:0.0001:1)*fc;
```

```

26 |
27 | w = 2*pi*f; % frequency range [rad/s]
28 |
29 | %% ————— Kalman SSM – NOMINAL—————
30 |
31 | Hs = 1; % significant wave height [m]
32 |
33 | gamma = 2; % peak enhancement factor. Realistic values are between 1
    | and 6.
34 |
35 | Tp = 10; % peak wave period [s].
36 |
37 | [S,sys_nom] = OPTIFUNCIONv2(w,Tp,Hs,gamma,dt); %Continuous Nominal
    | Model
38 |
39 | sys_t = c2d(sys_nom,dt);
40 | A_nom = sys_t.A; % To insert in Kalman filter
41 | B_nom = sys_t.B; % To insert in Kalman filter
42 | C_nom = sys_t.C; % To insert in Kalman filter
43 | D_nom = sys_t.D; % To insert in Kalman filter
44 |
45 | %% ————— External Spectrum – Plant—————
46 |
47 | Hs_pm = 1; % significant wave height [m]
48 |
49 | gamma_pm = 2; % peak enhancement factor
50 |
51 | Tp_pm = 10; % peak wave period [s].
52 |
53 | R = 0.001; % Measurement noise covariance
54 |
55 | %————— Continous Plan Model—————
56 |
57 | [S1,sys_plant] = OPTIFUNCIONv2(w,Tp_pm,Hs_pm,gamma_pm,dt);
58 |
59 | sys_plantd = c2d(sys_plant,dt);
60 |
61 | S_pm = sys_plantd; % Every plant must be called as S_pm
62 |
63 | %%————— Empty matrices to be filled —————
64 |
65 | x_estimate = zeros(4,length(t)); % Empty matrix to save estimated
    | states
66 |
67 | x_predicted = zeros(4,length(t)); % Empty matrix to save actual
    | states
68 |
69 | g = 1*randn(size(t)).'; % White noise – To set the below matrix sizes
70 |

```

```

71 random_reali=lsim(sys_t,g,t); % To set the below matrix sizes
72
73 [SDP_es,f1] = periodogram(random_reali,[],[],fs); % To set the above
    matrix sizes
74
75 l = 1000; % Number of iterations to create time series of random
    realisations
76
77 moy_k = zeros(length(SDP_es),l); %Empty matrix to insert all the
    values from the SDP_k
78
79 moy_p = zeros(length(SDP_es),l); %Empty matrix to insert all the
    values from the SDP_p
80
81 %% ----- To create random realisations -----
82 for a = 1:l
83
84 %% ----- White noise and input plant -----
85
86 % White noise and plant simulation are applied inside de loop to
    obtain
87 % each time a different random realisation and then average them.
88
89 g = 1*randn(size(t)); % White noise *****sensor
90
91 [y,~,x_p] = lsim(S_pm,g,t); % Plant + noise (Process noise) - Kalman
    input
92 v = sqrt(R)*randn(length(t),1);
93 x_p = x_p';
94 y_p = y+v;
95
96 %% ----- (Non-toolbox) Kalman Filter -----
97
98 Q = B_nom*B_nom.'; % Process noise covariance
99
100 y_estimated2 = zeros(length(t),1); % Empty matrix to save estimate
    values
101
102 yerror = zeros(length(t),1); % Empty matrix to save estimate values
103
104 L = zeros(4,length(t)); % Gain matrix
105
106 x = [0;0;0;0]; % Initial conditions for the states
107
108 x0 = [0;0;0;0]; % Initial conditions for the states
109
110 P = Q; % Process covariance matrix can be set as a non-zero value
111
112 % ----- Jacobians (Linearization part) -----

```

```

113
114 syms x1 x2 x3 x4
115
116 state = A_nom*[x1;x2;x3;x4];
117
118 response = C_nom*[x1;x2;x3;x4];
119
120 A_nom = jacobian(state,[x1,x2,x3,x4]); % Class = Sym
121 C_nom = jacobian(response,[x1,x2,x3,x4]); % Class = Sym
122
123 A_nom = double(A_nom); % Class = Double
124 C_nom = double(C_nom); % Class = Double
125
126 %% ----- State Space - Kalman -----
127
128 for k = 1:length(t)
129
130 % ----- 1 Calculate the gain -----
131 K = P*C_nom'/(C_nom*P*C_nom'+R); % Kalman Gain
132
133 % ----- 2 Calculate the current estimate -----
134 x = x + K*(y_p(k)-C_nom*x); % Current state estimate
135 x_estimate(:,k) = x; % To save state values
136 % y_predicted(k) = C_nom*x;
137
138 % ----- 3 Calculate the new error estimate P (Process Covariance
139 Matrix
140 P = (eye(4)-K*C_nom)*P; % Process Covariance Matrix (Error
141 estimate)
142 y_estimated2(k) = C_nom*x; % Current response estimate
143 L(:,k) = K; % Save the gain
144
145 % ----- Caculate the new error estimate -----
146 x = A_nom*x + B_nom*0; %Actual state at x_o conditions
147 P = A_nom*P*A_nom' + Q; % Update the new error estimate P
148
149 x_predicted(:,k) = x; % To save state values
150
151 end
152 [SDP_k,f_k] = periodogram(y_estimated2,[],[],fs); % SDF - Kalman
153 [SDP_es,f1] = periodogram(y_p,[],[],fs); % SDF - model input
154 moy_k(:,a) = SDP_k; % Send each value of SDF to this empty matrix
155 moy(:,a) = SDP_es; % Send each value of SDF to this empty matrix}
156 end
157 % mean_error = mean_error.^2;
158 % ECM(:,i) = mean(mean_error,2)
159 SDF_km = mean(moy_k,2); % Mean of several iteration of the SDP from
160 the Kalman filter

```

```

159 SDF_m = mean(moy,2); % Mean of several iteration of the SDP from the
      Model input
160 yerror = sum((yerror).^2)/length(yerror);
161
162 %%————— To plot kalman filter —————
163 figure
164 plot(t,L)
165 %————— Plot Target response vs Estimation Response—————
166 figure
167 subplot(3,1,1)
168 plot(t,y_p,'r',t,y_estimated2,'b--')
169 xlabel('Time ($s$)', 'Interpreter', 'latex', 'FontSize',12)
170 ylabel('Displacement ($m$)', 'Interpreter', 'latex', 'FontSize',12)
171 title('Estate Space Response – Random Realisations', 'Interpreter',
      'latex', 'FontSize',12)
172 legend('Target', 'Estimation')
173
174 %%————— To plot States and error states, response and error
      response—————
175
176 % dt_kalm = std(x_p(1,:));
177 % Plot State variable 1 vs Estimated state variable 1
178 subplot(4,1,1)
179 plot(t,x_p(1,:), 'r', t, x_predicted(1,:), 'b', t, (x_predicted(1,:)-x_p
      (1,:)), 'g--')
180 % yline(-dt_kalm*2); yline(dt_kalm*2)
181 xlabel('time ($s$)', 'Interpreter', 'latex', 'FontSize',12)
182 ylabel('$$x_1$$', 'Interpreter', 'latex', 'FontSize',12)
183 legend('Target', 'Estimation', '$$error_{x_1}$$', 'Interpreter', 'latex
      ', 'FontSize',9)
184 title(['Estate Space – State variables $$error_{x_1}$$ =', num2str(sum
      (abs(x_predicted(1,:)-x_p(1,:)))/length(x_p(1,:)))] , 'Interpreter
      ', 'latex', 'FontSize',12)
185 % Plot State variable 2 vs Estimated state variable 2
186 subplot(4,1,2)
187 plot(t,x_p(2,:), 'r', t, x_predicted(2,:), 'b', t, (x_predicted(2,:)-x_p
      (2,:)), 'g--')
188 xlabel('time (s)', 'Interpreter', 'latex', 'FontSize',12)
189 ylabel('$$\dot{x}_1$$', 'Interpreter', 'latex', 'FontSize',12)
190 legend('Target', 'Estimation', '$$error_{\dot{x}_1}$$', 'Interpreter', '
      latex', 'FontSize',9)
191 title(['$$error_{\dot{x}_1}$$ =', num2str(sum(abs(x_predicted(2,:)-x_p
      (2,:)))/length(x_p(2,:)))] , 'Interpreter', 'latex', 'FontSize',12)
192 % Plot State variable 3 vs Estimated state variable 3
193 subplot(4,1,3)
194 plot(t,x_p(3,:), 'r', t, x_predicted(3,:), 'b', t, (x_predicted(3,:)-x_p
      (3,:)), 'g--')
195 xlabel('time (s)', 'Interpreter', 'latex', 'FontSize',12)
196 ylabel('$$x_2$$', 'Interpreter', 'latex', 'FontSize',12)

```

```

197 legend('Target', 'Estimation', '$$error_{x_2}$$', 'Interpreter', 'latex
    ', 'FontSize', 9)
198 title(['$$error_{x_2}$$ =', num2str(sum(abs(x_predicted(3,:)-x_p(3,:))
    )/length(x_p(3,:)))], 'Interpreter', 'latex', 'FontSize', 12)
199 % Plot State variable 4 vs Estimated state variable 4
200 subplot(4,1,4)
201 plot(t,x_p(4,:), 'r', t, x_predicted(4,:), 'b', t, (x_predicted(4,:)-x_p
    (4,:)), 'g--')
202 xlabel('time (s)', 'Interpreter', 'latex', 'FontSize', 17)
203 ylabel('$$\dot{x}_2$$', 'Interpreter', 'latex', 'FontSize', 17)
204 dt_kalm = std(x_p(4,:));
205 CI = 1.96;
206 yline(-dt_kalm*CI); yline(dt_kalm*CI)
207 legend('Plan Model - Target', 'Kalman Filter - Estimated', '$$error_{\dot{x}_2}$$', 'Interpreter', 'latex', 'FontSize', 11)
208 title(['$$error_{\dot{x}_2}$$ =', num2str(sum(abs(x_predicted(4,:)-x_p
    (4,:)))/length(x_p(4,:)))], 'Interpreter', 'latex', 'FontSize', 17)
209
210
211
212 % ----- Plot Spectrum -----
213 figure
214 subplot(2,1,1)
215 % plot(f1,SDF_m, 'b--', f_k, SDF_km, 'g', f, S1, 'r-')
216 plot(f, S1, 'r', f1, SDF_m, 'b')
217 xlim([0 0.5])
218 xlabel('Frequency ($$Hz$$)', 'Interpreter', 'latex', 'FontSize', 17)
219 ylabel('SDF', 'Interpreter', 'latex', 'FontSize', 17)
220 title(['SDF obtained from the white noise realizations Hp =', num2str(Hs_pm), '
    $$\gamma$$ =', num2str(gamma_pm), ' Tp =', num2str(Tp_pm), '
    $$dt$$ =', num2str(dt)], 'Interpreter', 'latex', 'FontSize', 15)
221 % legend('Plant Model - Spectrum', 'Kalman Filter - Estimated Spectrum', 'Target Spectrum')
222 legend('Target Spectrum', 'Approximate Spectrum', 'Interpreter', 'latex
    ', 'FontSize', 11)
223
224 % ----- Plot Target response vs Estimation Response -----
225 subplot(2,1,2)
226 plot(t, y_p, 'r-', t, y_estimated2, 'b--', t, (y_estimated2-y_p), 'g--')
227 xlabel('Time ($$$s$$)', 'Interpreter', 'latex', 'FontSize', 17)
228 ylabel('$$\eta$$', 'Interpreter', 'latex', 'FontSize', 17)
229 dt_kalm = std(y);
230 CI = 1.96;
231 yline(-dt_kalm*CI); yline(dt_kalm*CI)
232 title('Estate Space Response - Random Realizations', ['Estimation
    Error =', num2str(sum(abs(y_estimated2-y_p))/length(y_p))], '
    Interpreter', 'latex', 'FontSize', 17)
233 legend('Plan Model - Target', 'Kalman Filter - Estimated', '$$error_y$$', 'Interpreter', 'latex', 'FontSize', 11)

```

```

234
235
236 %———— Plot Spectrum noisy/without noise————
237 figure
238 plot(t,y,'r',t,y_p,'b--')
239 xlabel('Time ($$$$)', 'Interpreter','latex','FontSize',17)
240 ylabel('$$\eta$$', 'Interpreter','latex','FontSize',17)
241 title('Random realisation Noise free/Noisy ', 'Interpreter','latex','
      FontSize',17)
242 legend('Noise free', 'Noisy', 'Interpreter','latex','FontSize',11)
243
244 %% This plot is to obtain SS response of the random realization, the
      SDF
245 % And \x_2 dot variable which correspond to the only controllable
      variable
246 % In the system
247
248 figure
249 subplot(3,1,1)
250 plot(t,y_p,'r-',t,y_estimated2,'b--',t,(y_estimated2-y_p),'g--')
251 xlabel('Time ($$$$)', 'Interpreter','latex','FontSize',17)
252 ylabel('$$\eta$$', 'Interpreter','latex','FontSize',17)
253 dt_kalm = std(y);
254 CI = 1.96;
255 yline(-dt_kalm*CI); yline(dt_kalm*CI)
256 title('a) Estate Space Response – Random Realizations ', [' Estimation
      Error =', num2str(sum(abs(y_estimated2-y_p))/length(y_p))], '
      Interpreter','latex','FontSize',17)
257 legend('Plan Model – Target', 'Kalman Filter – Estimated', '
      $$error_y$$', 'Interpreter','latex','FontSize',11)
258
259 subplot(3,1,2)
260 plot(f,S1,'r',f_k,SDF_km,'b--')
261 xlim([0 0.5])
262 xlabel('Frequency ($$Hz$$)', 'Interpreter','latex','FontSize',17)
263 ylabel('SDF', 'Interpreter','latex','FontSize',17)
264 title(['b) SDF obtained from the white noise realizations Hs =',
      num2str(Hs_pm), ' $$\gamma$$ =', num2str(gamma_pm), ' Tp =', num2str(
      Tp_pm), ' $$dt$$ =', num2str(dt)], 'Interpreter','latex','FontSize
      ',17)
265 % legend('Plant Model – Spectrum', 'Kalman Filter – Estimatiated
      Spectrum', 'Target Spectrum')
266 legend('Plant Model – Target Spectrum', 'Kalman Filter – Estimatiated
      Spectrum', 'JONSWAP ALGORIHM', 'Interpreter','latex','FontSize',11)
267
268 subplot(3,1,3)
269 plot(t,x_p(4,:), 'r', t, x_predicted(4,:), 'b', t, (x_predicted(4,:) - x_p
      (4,:)), 'g--')
270 xlabel('time (s)', 'Interpreter','latex','FontSize',17)

```

```
271 ylabel('$$\dot{x}_2$$', 'Interpreter', 'latex', 'FontSize', 17)
272 dt_kalm = std(x_p(4, :));
273 CI = 1.96;
274 yline(-dt_kalm*CI); yline(dt_kalm*CI)
275 legend('Plan Model - Target', 'Kalman Filter - Estimated', '$$error_{\dot{x}_2}$$', 'Interpreter', 'latex', 'FontSize', 11)
276 title(['c' '$$error_{\dot{x}_2}$$ =', num2str(sum(abs(x_predicted(4, :)) - x_p(4, :)))/length(x_p(4, :))], 'Interpreter', 'latex', 'FontSize', 17)
```

## Appendix C

# Least-Squares MATLAB code implementation

```
1 function [S1,sys_c] = OPTIFUNCIONv2(w,Tp_pm,Hs_pm,gamma_pm,dt)
2
3 %% ----- JONSWAP Spectrum -----
4 nw=length(w);
5 f=w/(2.*pi);
6 A=0.3125*Hs_pm^2/Tp_pm^4;
7 B=1.25/Tp_pm^4;
8 fp=1./Tp_pm;
9 m0=0.;
10 m_1=0.;
11 Pwave=0.;
12 Hw=zeros(1,nw);
13 S1=zeros(1,nw);
14 for i=2:nw
15     fc=0.5*(f(i)+f(i-1));
16     df=f(i)-f(i-1);
17     S1(i)=A/fc^5*exp(-B/fc^4);
18     if (fc<fp)
19         sigma=0.07;
20     else
21         sigma=0.09;
22     end
23     pa=exp(-(fc-fp)^2/(2.*sigma^2*fp^2));
24     S1(i)=S1(i)*gamma_pm^pa;
25     m0=m0+S1(i)*df;
26     m_1=m_1+S1(i)/fc*df;
27 end
28 alpha=Hs_pm^2/(16.*m0);
```

```

29 Te=m_1/m0;
30 for i=2:nw
31     df=f(i)-f(i-1);
32     S1(i)=S1(i)*alpha;
33     Hw(i)=sqrt(2.*S1(i)*df);
34     Pwave=Pwave+0.25*1025.*9.81*9.81*Hw(i)*Hw(i)/w(i);
35 end
36 %% LPF
37 digFilt=designfilt('lowpassfir','PassbandFrequency',0.95,'
    StopbandFrequency',2,'PassbandRipple',1,'StopbandAttenuation',60,'
    SampleRate',100);
38 S1 = filter(digFilt,S1);
39
40
41 % ----- LS -----
42 ydata1 = S1;
43 x = w;
44
45 % Optimized variables
46 G1 = optimvar('G','LowerBound',0)
47 k1 = optimvar('k',2,'LowerBound',0)
48 c1 = optimvar('c',2,'LowerBound',0)
49
50 % -----JONSWAP Spectrum function-----
51
52 fun1 = ((G1).*x.^4)./(((x.^2-k1(1)).^2+(c1(1).*x).^2).*(((x.^2)-k1(2)
    ).^2 ...
53     +(c1(2).*x).^2)); % Fourth order filter
54 obj1 = sum((ydata1 - fun1).^2); % Least-Squares
55
56 lsqproblem1 = optimproblem("Objective",obj1); % Solving LSQ function
57
58 % Initial valuables
59 x1.G = [6.183];
60 x1.k = [0.398 1.794];
61 x1.c = [0.085 2.709];
62
63 % x1.G = [rand];
64 % x1.k = [rand rand];
65 % x1.c = [rand rand];
66
67 % Solving the optimization problem
68 show(lsqproblem1) %Shows the LS optimization problem
69 [sol1,fval1] = solve(lsqproblem1,x1,'solver','fmincon')
70 disp(sol1.G)
71 disp(sol1.k)
72 disp(sol1.c)
73
74 % Save the new coefficients

```

```

75 x1.G = sol1.G
76 x1.k = sol1.k
77 x1.c = sol1.c
78
79 figure
80 respondedata = evaluate(fun1, sol1);
81 plot(f, ydata1, 'r--', f, respondedata, 'b--'); hold on;
82 xlim([0 0.5])
83 legend('Target spectrum', 'Approximate Spectrum')
84 xlabel('Frequency ($Hz$)', 'Interpreter', 'latex', 'FontSize', 17)
85 ylabel('SDF', 'Interpreter', 'latex', 'FontSize', 17)
86 title(['SDF obtained from LS Hs =', num2str(Hs_pm), ' $$$\gamma$$$ =',
      num2str(gamma_pm), ' Tp =', num2str(Tp_pm), ' $$$dt$$$ =', num2str(dt)
      ], 'Interpreter', 'latex', 'FontSize', 17)
87 hold on
88 grid on
89
90 %-----State Space model-----
91
92 % Cascading Two second order filters
93
94 % First filter
95 A_1_a = [0 1; -x1.k(1) -x1.c(1)];
96 B_1_a = [0; 1];
97 C_1_a = [0 1];
98 D_1_a = zeros(2,1);
99 % Second filter
100 A_2_a = [0 1; -x1.k(2) -x1.c(2)];
101 B_2_a = sqrt(x1.G) .* [0; 1];
102 C_2_a = [0 1];
103 D_2_a = zeros(2,1);
104 % ABCD state space form
105 A_a = [A_1_a zeros(2,2); B_2_a.*C_1_a A_2_a];
106 B_a = [B_1_a; D_1_a];
107 C_a = [zeros(1,2) C_2_a];
108 D_a = 0;
109
110 sys_c = ss(A_a, B_a, C_a, D_a); % State- Space Coninuous
111 end

```

# Bibliography

- [1] P-T. D. Spanos. «ARMA Algorithms for Ocean Wave Modeling». In: *Journal of Energy Resources Technology-transactions of The Asme* 105 (1983), pp. 300–309 (cit. on p. 2).
- [2] Kjell Budal and Johannes Falnes. «Status 1983 of the Norwegian wave-power buoy project». In: 1983 (cit. on p. 2).
- [3] M.K. Ochi. *Ocean Waves: The Stochastic Approach*. Cambridge Ocean Technology Series. Cambridge University Press, 1998. ISBN: 9780521563789 (cit. on pp. 5, 6).
- [4] Rebecca Hummels. «Introduction into Physical Oceanography». In: *Handbook on Marine Environment Protection : Science, Impacts and Sustainable Management*. Ed. by Markus Salomon and Till Markus. Cham: Springer International Publishing, 2018, pp. 3–35. ISBN: 978-3-319-60156-4. DOI: 10.1007/978-3-319-60156-4\_1. URL: [https://doi.org/10.1007/978-3-319-60156-4\\_1](https://doi.org/10.1007/978-3-319-60156-4_1) (cit. on p. 6).
- [5] Willard J. Pierson Jr. and Lionel Moskowitz. «A proposed spectral form for fully developed wind seas based on the similarity theory of S. A. Kitaigorodskii». In: *Journal of Geophysical Research (1896-1977)* 69.24 (1964), pp. 5181–5190. DOI: <https://doi.org/10.1029/JZ069i024p05181> (cit. on p. 6).
- [6] M.K. Ochi. *Ocean Waves: The Stochastic Approach*. Cambridge Ocean Technology Series. Cambridge University Press, 1998, pp 18. ISBN: 9780521563789 (cit. on p. 7).
- [7] K.J. Astrom, K.J.A. m, trKarl Johan, and Inc Autodesk. *Introduction to Stochastic Control Theory*. Mathematics in Science and Engineering. Elsevier Science, 1970. ISBN: 9780120656509 (cit. on p. 7).
- [8] P.A. Gagniuc. *Markov Chains: From Theory to Implementation and Experimentation*. John Wiley & Sons, 2017. ISBN: 9781119387596 (cit. on p. 8).

- [9] F.M. Dekking, C. Kraaikamp, H.P. Lopuhaä, and L.E. Meester. *A Modern Introduction to Probability and Statistics: Understanding Why and How*. Springer Texts in Statistics. Springer, 2005. ISBN: 9781852338961 (cit. on pp. 8, 10).
- [10] Andrey G. Cherstvy, Aleksei V. Chechkin, and Ralf Metzler. «Anomalous diffusion and ergodicity breaking in heterogeneous diffusion processes». In: *New Journal of Physics* 15 (2013) (cit. on p. 8).
- [11] M.K. Ochi. *Ocean Waves: The Stochastic Approach*. Cambridge Ocean Technology Series. Cambridge University Press, 1998, pp 13–15. ISBN: 9780521563789 (cit. on p. 9).
- [12] H.P. Hsu. *Schaum's Outline of Probability, Random Variables, and Random Processes, Fourth Edition*. McGraw-Hill Education, 2019. ISBN: 9781260453812 (cit. on p. 10).
- [13] MATLAB. *version 7.10.0 (R2022a)*. Natick, Massachusetts: The MathWorks Inc., 2022 (cit. on p. 11).
- [14] K. Ogata. *Modern Control Engineering*. Instrumentation and controls series. Prentice Hall, 2010, pp. 675–676. ISBN: 9780136156734 (cit. on p. 11).
- [15] C. Guedes Soares and Z. Cherneva. «Spectrogram analysis of the time–frequency characteristics of ocean wind waves». In: *Ocean Engineering* 32.14 (2005), pp. 1643–1663. ISSN: 0029-8018. DOI: <https://doi.org/10.1016/j.oceaneng.2005.02.008>. URL: <https://www.sciencedirect.com/science/article/pii/S0029801805000806> (cit. on p. 12).
- [16] Greg Welch and Gary Bishop. «An Introduction to the Kalman Filter». In: *Proc. Siggraph Course* 8 (Jan. 2006), p. 2 (cit. on p. 12).
- [17] Greg Welch and Gary Bishop. «An Introduction to the Kalman Filter». In: *Proc. Siggraph Course* 8 (Jan. 2006), p. 5 (cit. on p. 14).
- [18] P.-T.D. SPANOS. «Filter Approaches to Wave Kinematics Approximation». In: *Random Vibration-Status and Recent Developments*. Ed. by I. Elishakoff and R.H. Lyon. Vol. 14. Studies in Applied Mechanics. Elsevier, 1986, pp. 459–473. DOI: <https://doi.org/10.1016/B978-0-444-42665-9.50033-5> (cit. on p. 17).
- [19] P-T. D. Spanos. «ARMA Algorithms for Ocean Wave Modeling». In: *Journal of Energy Resources Technology* 105.3 (Sept. 1983), pp. 300–309. ISSN: 0195-0738. DOI: [10.1115/1.3230919](https://doi.org/10.1115/1.3230919). URL: <https://doi.org/10.1115/1.3230919> (cit. on p. 17).

- [20] J.T. Scruggs, S.M. Lattanzio, A.A. Taflanidis, and I.L. Cassidy. «Optimal causal control of a wave energy converter in a random sea». In: *Applied Ocean Research* 42 (2013), pp. 1–15. ISSN: 0141-1187. DOI: <https://doi.org/10.1016/j.apor.2013.03.004>. URL: <https://www.sciencedirect.com/science/article/pii/S0141118713000205> (cit. on p. 24).